

---

# HYPERGRAPH NEURAL NETWORKS THROUGH THE LENS OF MESSAGE PASSING: A COMMON PERSPECTIVE TO HOMOPHILY AND ARCHITECTURE DESIGN

Lev Telyatnikov<sup>1</sup>, Maria Sofia Bucarelli<sup>1</sup>, Guillermo Bernardez<sup>2</sup>,  
 Olga Zaghen<sup>3</sup>, Simone Scardapane<sup>1</sup>, Pietro Liò<sup>4</sup>  
 Sapienza University of Rome<sup>1</sup>, UPC Barcelona<sup>2</sup>,  
 University of Trento<sup>3</sup>, University of Cambridge<sup>4</sup>

## ABSTRACT

Most of the current hypergraph learning methodologies and benchmarking datasets in the hypergraph realm are obtained by *lifting* procedures from their graph analogs, simultaneously leading to overshadowing hypergraph network foundations. This paper attempts to confront some pending questions in that regard: Can the concept of homophily play a crucial role in Hypergraph Neural Networks (HGNNs), similar to its significance in graph-based research? Is there room for improving current hypergraph architectures and methodologies? (e.g. by carefully addressing the specific characteristics of higher-order networks) Do existing datasets provide a meaningful benchmark for HGNNs? Diving into the details, this paper proposes a novel conceptualization of homophily in higher-order networks based on a message passing scheme; this approach harmonizes the analytical frameworks of datasets and architectures, offering a unified perspective for exploring and interpreting complex, higher-order network structures and dynamics. Further, we propose MultiSet, a novel message passing framework that redefines HGNNs by allowing hyperedge-dependent node representations, as well as introduce a novel architecture –MultiSetMixer– that leverages a new hyperedge sampling strategy. Finally, we provide an extensive set of experiments that contextualize our proposals and lead to valuable insights in hypergraph representation learning.

## 1 INTRODUCTION

Hypergraph learning techniques have rapidly grown in recent years, demonstrating their effectiveness in processing higher-order interactions in numerous fields, spanning from recommender systems (Yu et al., 2021; Zheng et al., 2018; La Gatta et al., 2022), to bioinformatics (Zhang et al., 2018; Yadati et al., 2020; Klamt et al., 2009) and computer vision (Li et al., 2022a; Xu et al., 2022; Gao et al., 2012; Yin et al., 2017; Kim et al., 2011). However, so far, the development of HyperGraph Neural Networks (HGNNs) has been largely influenced by the well-established Graph Neural Network (GNN) field. In fact, most of the current methodologies and benchmarking datasets in the hypergraph realm are obtained by *lifting* procedures from their graph counterparts.

Drawing inspiration from graph-based models has significantly propelled the advancement of hypergraph research (Feng et al., 2019; Yadati et al., 2019; Chien et al., 2022), and it has simultaneously led to overshadowing hypergraph network foundations. We argue that it is now the time to address fundamental questions in order to pave the way for further innovative ideas in the field. In that regard, this study explores some of these open questions to understand better current HGNN architectures and benchmarking datasets. Can the concept of homophily play a crucial role in HGNNs, similar to its significance in graph-based research? Given that current HGNNs are predominantly extensions of GNN architectures adapted to the hypergraph domain, are these extended methodologies suitable, or should we explore new strategies tailored specifically for handling hypergraph-based data? Are the existing hypergraph benchmarking datasets truly *meaningful* and representative enough to draw robust and valid conclusions?

---

To begin with, we explore how the concept of homophily can be characterized in complex, higher-order networks. Notably, there are many ways of characterizing homophily in hypergraphs –such as the distribution of node features, the analogous distribution of the labels, or the group connectivity similarity (as already discussed in (Veldt et al., 2023)). In particular, this work places the *node class distribution* at the core of the analysis, and introduces a novel definition of homophily that relies on a message passing scheme. Interestingly, this enables us to analyze both hypergraph datasets and architecture designs from the same perspective. In fact, we reckon that this unified message passing framework has the potential to inspire the development of meaningful contributions for processing higher-order relationships more effectively.

Next, we study state-of-the-art HGNN architectures and introduce a new framework called MultiSet. We demonstrate that MultiSet generalizes most existing frameworks for HGNNs, including AllSet (Chien et al., 2022) and UniGCNII (Huang & Yang, 2021). Our framework presents an innovative approach to message passing, where multiple hyperedge-dependent representations of nodes are enabled. Then, we introduce novel methodologies to process hypergraphs –including MultiSetMixer, a new HGNN architecture based on a particular implementation of a MultiSet layer. In these implementations, we introduce a novel connectivity-based mini-batching strategy capable of processing large hyperedges and discuss the intriguing property of natural connectivity-based distribution shifts.

Last, but not least, we provide an extensive set of experiments that, driven by the general questions stated above, aim to gain a better understanding on fundamental aspects of hypergraph representation learning. In fact, the obtained results not only help us contextualize the proposals introduced in this work, but indeed offer valuable insights that might help improve future hypergraph approaches.

## 2 RELATED WORKS

**Homophily in hypergraphs.** Homophily measures are typically defined for graph models and consider only pairwise relationships. In the context of Graph Neural Networks (GNNs), many of the current models implicitly use the homophily assumption, which is shown to be crucial for achieving a robust performance with relational data (Zhou et al., 2020; Chien et al., 2020; Halcrow et al., 2020). Nevertheless, despite the pivotal role that homophily plays in graph representation learning, its hypergraph counterpart mainly remains unexplored. In fact, to the best of our knowledge, Veldt et al. (2023) is the only work that faces the challenge of defining homophily in higher-order networks. Veldt et al. (2023) introduces a framework in which hypergraphs are used to quantify homophily from group interactions; however, the definition of homophily is restricted to uniform hypergraphs –i.e. where all hyperedges have exactly the same size (more details in Section 3). This represents a hard assumption that complicates its applicability to most of the current hypergraph datasets.

**Hypergraph Neural Networks.** The work of Chien et al. (2022) introduced AllSet, a general framework to describe HGNNs through a two-step message passing based mechanism, and demonstrated that most of the current hypergraph models are special instances of their formulation, based on the composition of two learnable permutation invariant functions that transmit information from nodes to hyperedges, and back from hyperedges to nodes. In particular, AllSet can be seen as a generalization of the most commonly used HGNNs, including all clique expansion based (CE) methods, HGNN (Feng et al., 2019), HNHN (Dong et al., 2020), HCHA (Bai et al., 2021), HyperSAGE (Arya et al., 2020) and HyperGCN (Yadati et al., 2019). Chien et al. (2022) also proposes two novel AllSet-like learnable layers: the first one –AllDeepSet– exploits Deep Set (Zaheer et al., 2017), and the second one –AllSetTransformer– Set Transformer (Lee et al., 2019), both of them achieving state-of-the-art results in the most common hypergraph benchmarking datasets. Concurrent to AllSet, the work of Huang & Yang (2021) also aimed at designing a common framework for graph and hypergraph NNs, and its more advanced UniGCNII method leverages initial residual connections and identity mappings in the hyperedge-to-node propagation to address over-smoothing issues; notably, UniGCNII do not fall under AllSet notation due to these residual connections. With Chien et al. (2022) and Huang & Yang (2021) being the most relevant ones to our work, we extend this review in Appendix A.

**Notation.** A hypergraph is an ordered pair of sets  $\mathcal{G} = (\mathcal{V}, \mathcal{E})$ , where  $\mathcal{V}$  is the set of nodes and  $\mathcal{E}$  is the set of hyperedges. Each hyperedge  $e \in \mathcal{E}$  is a subset of  $\mathcal{V}$ , i.e.,  $e \subseteq \mathcal{V}$ . A hypergraph is a generalization of the concept of a graph where (hyper)edges can connect more than two nodes. A vertex  $v$  and a hyperedge  $e$  are said to be incident if  $v \in e$ . For each node  $v$ , we denote its class by  $y_v$ , and by  $\mathcal{E}_v = \{e \in \mathcal{E} : v \in e\}$  the subset of hyperedges in which it is contained, with  $d_v = |\mathcal{E}_v|$  depicting the node degree. The set of classes of the hypergraph is represented by  $\mathcal{C} = \{c_i\}_{i=1}^{|\mathcal{C}|}$ .

### 3 DEFINING AND MEASURING HOMOPHILY IN HYPERGRAPHS

Homophily is a graph property that describes the tendency for edges to connect nodes that are similar (Moody, 2001; Shrum et al., 1988; Verbrugge, 1983). Currently, the most common measure of graph homophily is the proportion of edges that connect nodes of the same class. In pairwise relationships, a high degree of network homophily tends to create a network with communities, based on nodes’ class, that are highly connected within each other and poorly connected to the outside. Extending the concept of homophily to higher-order interactions is not straightforward, but it becomes crucial in order to avoid discarding valuable information about the composition of groups in which individuals participate. In this Section, we recap the general notion of higher-order homophily for  $k$ -uniform hypergraphs introduced in (Veldt et al., 2023) and present a novel propagation-based homophily measure which is applicable for general, non-uniform hypergraphs. In essence, the score proposed in Veldt et al. (2023) tends to primarily assess the composition of hyperedges within the graph by quantifying the distribution of classes among hyperedges. In contrast, our definition places a greater emphasis on capturing the interconnections between different hyperedges by the exchange of information between nodes following the message passing scheme.

**$k$ -uniform Homophily** Veldt et al. (2023) defines general higher-order homophily for  $k$ -uniform hypergraphs  $G_k = (\mathcal{V}, \mathcal{E}_k)$  which we refer to as  *$k$ -uniform homophily*. The type  $t$ -affinity score for each  $t \in \{1, \dots, k\}$ , indicates the likelihood of a node belonging to class  $c$  participating in hyperedges in which exactly  $t$  group members belong to class  $c$ . The authors introduce a *baseline score* that measures the probability that a class- $c$  node is in a hyperedge where  $t$  members are from class  $c$ , given that the other  $k - 1$  nodes were chosen uniformly at random. The  $k$ -uniform hypergraph homophily measure can be expressed as a ratio of affinity and baseline scores, with a ratio value of 1 indicating that the group is formed uniformly at random, while any other number indicates that group interactions are either overexpressed or underexpressed for class  $c$ . Note that non-uniform hypergraphs cannot directly be evaluated with  $k$ -uniform homophily scores; instead, the corresponding initial hyperedge set  $\mathcal{E}$  has to be restricted to particular  $k$ -uniform hyperedges, and for each  $k$  values they are processed separately. The detailed formulation of homophily measures and corresponding plots for each dataset can be found in Appendix J.

**Message Passing Homophily** We present a novel two-step message passing homophily measure that, unlike the one proposed by Veldt et al. (2023), does not assume a  $k$ -uniform hypergraph structure. Furthermore, the proposed measure enables the definition of a score for each node and hyperedge for any neighborhood resolution, i.e., the connectivity of the hypergraph can be explicitly investigated. Our homophily definition follows the two-step message passing mechanism starting from the hyperedges of the hypergraph. Thus, given an edge  $e$ , we define the 0-level hyperedge homophily  $h_e^0(c)$  as the fraction of nodes within each hyperedge that belong to class  $c$ , i.e.

$$h_e^0(c) = \frac{1}{|e|} \sum_{v \in e} \mathbb{1}_{y_v=c}. \quad (1)$$

This score describes how homophilic the initial connectivity is with respect to class  $c$ . By computing the score for every class  $c_i \in \mathcal{C}$  we obtain a categorical distribution for each hyperedge  $e \in \mathcal{E}$ , i.e.  $h_e^0 = (h_e^0(c_0), \dots, h_e^0(c_{|\mathcal{C}|}))$ . We can then use this 0-level homophily information as a starting point to calculate higher-level homophily measurements for both nodes and hyperedges through the two-step message passing approach. Formally, we define the  $t$ -level homophily score as

$$h_v^t(y_v) = \text{AGG}_{\mathcal{E}} (\{h_e^{t-1}(y_v)\}_{e \in \mathcal{E}_v}), \quad (2) \quad h_e^t(c) = \text{AGG}_{\mathcal{V}} (\{h_v^{t-1}\}_{v \in e}), \quad (3)$$

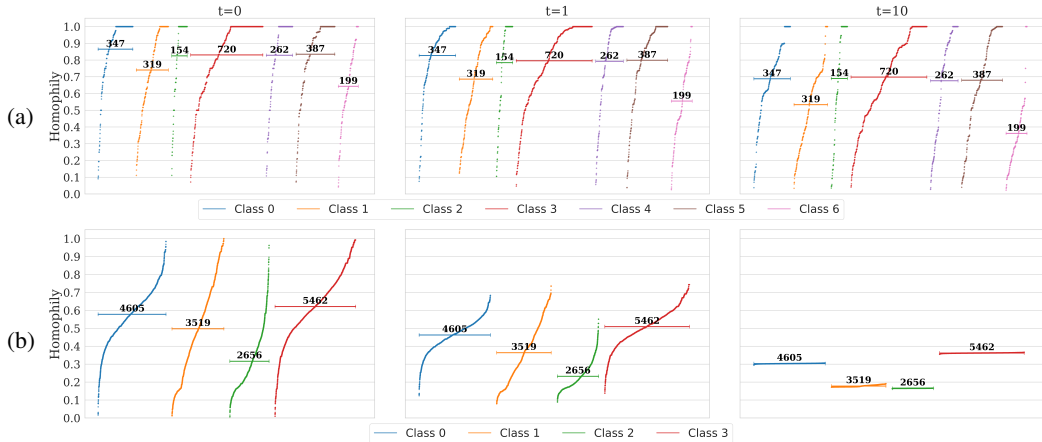


Figure 1: Node Homophily Distribution Scores for CORA-CA (a) and 20Newsgroups (b) using Equation 2 at  $t = 0, 1,$  and  $10$  (left, middle, and right plots correspondingly). Horizontal lines depict class mean homophily, with numbers above indicating the number of visualized points per class.

where  $AGG_{\mathcal{E}}$  and  $AGG_{\mathcal{V}}$  are functions that aggregate edge and node homophily scores, respectively. In our implementation, we considered the mean operation for both aggregations.

**Qualitative Analysis** In this paragraph, we are taking a closer look at the qualitative analysis of the node homophily measure we introduced. One of the most straightforward ways to make use of the message passing homophily measure is to visualize how the node homophily score, as described in Eq. 2, changes dynamically. We’ve depicted this process in Figure 1, focusing on the CORA-CA and 20NewsGroup datasets. Please note that in the figure, we are only showing non-isolated nodes. Looking at Figure 1 (a), we can observe several notable trends. First, in the initial node distribution ( $t = 0$ ), every class, except class 6, has a significant number of fully homophilic nodes. As we move to the 1-hop neighborhood ( $t = 1$ ), the corresponding classes either exhibit a moderate decrease in homophily or show no decrease at all. It’s worth noting that at  $t = 0, 1,$  and  $10$ , class 2 maintains a stable homophily distribution, hinting at an isolated subnetwork within. Furthermore, at  $t = 10$ , some points still maintain a node homophily score of 1, indicating the presence of multiple small subnetworks. Class 6 consistently displays the lowest average homophily measure at every step, with an average score of approximately 38% at  $t = 10$ . The node homophily distribution for the 20Newsgroups dataset is visualized in Figure 1 (b). At time step  $t = 0$ , we observe a wide range of homophily scores from 0 to 1 for each class. This suggests that the network is highly irregular with respect to connectivity. Moving to time step  $t = 1$ , there is a significant decrease in the homophily scores for every class, indicating a high degree of heterophily within the 1-hop neighborhood, which is not surprising considering step zero node homophily distribution. Finally, at time step  $t = 10$ , we can observe that all the classes converge to approximately the same homophily values within each class. This convergence suggests that the network is highly interconnected. More insights regarding node homophily measure and related HGNNs performances are described in Section 5 while the rest of the plots for the datasets can be found in Appendix I.

## 4 METHODS

Current HGNNs aim to generalize GNN concepts to the hypergraph domain, and are specially focused on redefining graph-based propagation rules to accommodate higher-order structures. In this regard, the work of Chien et al. (2022) introduced a general notation framework, called AllSet, that encompasses most of the currently available HGNN layers, including CEGCN/CEGAT, HGNN (Feng et al., 2019), HNHN (Dong et al., 2020), HCHA (Bai et al., 2021), HyperGCN (Yadati et al., 2019), and the AllDeepSet and AllSetTransformer presented in the same work (Chien et al., 2022).

The first part of this Section revisits the original AllSet formulation. Then, we introduce a new framework –termed MultiSet– which extends AllSet by allowing multiple hyperedge-dependent

representations of nodes. Finally, we present some novel methodologies to process hypergraphs—including MultiSetMixer, a new HGNN architecture within the MultiSet framework.

#### 4.1 ALLSET PROPAGATION SETTING

For a given node  $v \in \mathcal{V}$  and hyperedge  $e \in \mathcal{E}$  in a hypergraph  $\mathcal{G} = (\mathcal{V}, \mathcal{E})$ , let  $\mathbf{x}_v^{(t)} \in \mathbb{R}^f$  and  $\mathbf{z}_e^{(t)} \in \mathbb{R}^d$  denote their vector representations at propagation step  $t$ . We say that a function  $f$  is a multiset function if it is permutation invariant w.r.t. each of its arguments in turn. Typically,  $\mathbf{x}_v^{(0)}$  and  $\mathbf{z}_e^{(0)}$  are initialized based on the corresponding node and hyperedge original features, if available. The vectors  $\mathbf{x}_v^{(0)}$  and  $\mathbf{z}_e^{(0)}$  represent the initial node and hyperedge features, respectively. In this context, the AllSet framework (Chien et al., 2022) consists in the following two-step update rule:

$$\mathbf{z}_e^{(t+1)} = f_{\mathcal{V} \rightarrow \mathcal{E}}(\{\mathbf{x}_u^{(t)}\}_{u:u \in e}; \mathbf{z}_e^{(t)}), \quad (4)$$

$$\mathbf{x}_v^{(t+1)} = f_{\mathcal{E} \rightarrow \mathcal{V}}(\{\mathbf{z}_e^{(t+1)}\}_{e \in \mathcal{E}_v}; \mathbf{x}_v^{(t)}), \quad (5)$$

where  $f_{\mathcal{V} \rightarrow \mathcal{E}}$  and  $f_{\mathcal{E} \rightarrow \mathcal{V}}$  are two permutation invariant functions with respect to their first input. Equations 4 and 5 describe the propagation from nodes to hyperedges and from hyperedges to nodes, respectively. We extend the original AllSet formulation to accommodate UniGCNII (Huang & Yang, 2021), a concurrent work to AllSet, by modifying the node update rule (Eq. 5) in order to allow residual connections, i.e.:

$$\mathbf{x}_v^{(t+1)} = f_{\mathcal{E} \rightarrow \mathcal{V}}(\{\mathbf{z}_e^{(t+1)}\}_{e \in \mathcal{E}_v}; \{\mathbf{x}_v^{(k)}\}_{k=0}^t). \quad (6)$$

There is no requirement for the function to be permutation invariant with respect to this second set.

**Proposition 1.** *UniGCNII Huang & Yang, 2021 is a special case of AllSet considering 4 and 6.*

In the practical implementation of a model,  $f_{\mathcal{V} \rightarrow \mathcal{E}}$  and  $f_{\mathcal{E} \rightarrow \mathcal{V}}$  are parametrized and learnt for each dataset and task, and particular choices of these functions give rise to the different HGNN layer architectures considered in this paper; more details in Appendix B.

#### 4.2 MULTISSET FRAMEWORK

In this Section, we introduce our proposed MultiSet framework, which can be seen as an extension of AllSet where nodes can have multiple co-existing hyperedge-based representations. For a given hyperedge  $e \in \mathcal{E}$  in a hypergraph  $\mathcal{G} = (\mathcal{V}, \mathcal{E})$ , we denote by  $\mathbf{z}_e^{(t)} \in \mathbb{R}^d$  its vector representation at step  $t$ . However, for a node  $v \in \mathcal{V}$ , MultiSet allows for as many representations of the node as the number of hyperedges it belongs to. We denote by  $\mathbf{x}_{v,e}^{(t)} \in \mathbb{R}^f$  the vector representation of node  $v$  in a hyperedge  $e \in \mathcal{E}_v$  at propagation time  $t$ , and by  $\mathbb{X}_v^{(t)} = \{\mathbf{x}_{v,e}^{(t)}\}_{e \in \mathcal{E}_v}$  the set of all  $d_v$  hidden states of that node in the specified time-step. Accordingly, the hyperedge and node update rules of MultiSet are formulated to accommodate hyperedge-dependent node representations:

$$\mathbf{z}_e^{(t+1)} = f_{\mathcal{V} \rightarrow \mathcal{E}}(\{\mathbb{X}_u^{(t)}\}_{u:u \in e}; \mathbf{z}_e^{(t)}), \quad (7)$$

$$\mathbf{x}_{v,e}^{(t+1)} = f_{\mathcal{E} \rightarrow \mathcal{V}}(\{\mathbf{z}_e^{(t+1)}\}_{e \in \mathcal{E}_v}; \{\mathbb{X}_v^{(k)}\}_{k=0}^t), \quad (8)$$

where  $f_{\mathcal{V} \rightarrow \mathcal{E}}$  and  $f_{\mathcal{E} \rightarrow \mathcal{V}}$  are two multiset functions with respect to their first input. After  $T$  iterations of message passing, MultiSet also considers a last readout-based step with the idea of obtaining a unique final representation  $\mathbf{x}_v^T \in \mathbb{R}^{f'}$  for each node from the set of its hyperedge-based representations:

$$\mathbf{x}_v^T = f_{\mathcal{V} \rightarrow \mathcal{V}}(\{\mathbb{X}_v^{(k)}\}_{k=0}^T) \quad (9)$$

where  $f_{\mathcal{V} \rightarrow \mathcal{V}}$  is also a multiset function.

**Proposition 2.** *AllSet 4-5, as well as its extension 4-6, are special cases of MultiSet 7-8-9.*

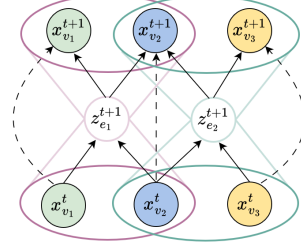


Figure 2: AllSet layout

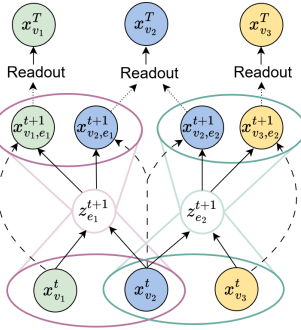


Figure 3: MultiSet layout

---

### 4.3 TRAINING MULTISSET NETWORKS

This Section describes the main characteristics of our MultiSet layer implementation, termed MultiSetMixer, and presents a novel sampling procedure that our model incorporates.

**Learning MultiSet Layers** Following the mixer-style block designs (Tolstikhin et al., 2021) and standard practice, we propose the following MultiSet layer implementation for HGNNs:

$$\mathbf{z}_e^{(t+1)} = f_{\mathcal{V} \rightarrow \mathcal{E}}(\{\mathbf{x}_{u,e}^{(t)}\}_{u:u \in e}; \mathbf{z}_e^{(t)}) := \frac{1}{|e|} \sum_{v \in e} \mathbf{x}_{v,e}^{(t)} + \text{MLP} \left( \text{LN} \left( \frac{1}{|e|} \sum_{v \in e} \mathbf{x}_{v,e}^{(t)} \right) \right), \quad (10)$$

$$\mathbf{x}_{v,e}^{(t+1)} = f_{\mathcal{E} \rightarrow \mathcal{V}}(\mathbf{z}_e^{(t+1)}; \mathbf{x}_{v,e}^{(t)}) := \mathbf{x}_{v,e}^{(t)} + \text{MLP} \left( \text{LN}(\mathbf{x}_{v,e}^{(t)}) \right) + \mathbf{z}_e^{(t+1)}, \quad (11)$$

$$\mathbf{x}_v^{(T)} = f_{\mathcal{V} \rightarrow \mathcal{V}}(\mathbb{X}_v^{(T)}) := \frac{1}{d_v} \sum_{e \in \mathcal{E}_v} \mathbf{x}_{v,e}^{(t)} \quad (12)$$

where MLPs are composed of two fully-connected layers, and LN stands for layer normalisation. This novel architecture, which we call MultiSetMixer, is based on a mixer-based pooling operation for (i) updating hyperedges from its node’s representations, and (ii) generate and update hyperedge-dependent representations of the nodes.

**Proposition 3.** *The functions  $f_{\mathcal{V} \rightarrow \mathcal{E}}$ ,  $f_{\mathcal{E} \rightarrow \mathcal{V}}$  and  $f_{\mathcal{V} \rightarrow \mathcal{V}}$  defined in MultiSetMixer are permutation invariant. Furthermore, these functions are universal approximators of multiset functions when the size of the input multiset is finite.*

**Mini-batching** The motivation for introducing a new strategy to iterate over hypergraph datasets is twofold. On the one hand, current HGNN pipelines suffer from scalability issues to process large datasets and very large hyperedges. On the other, pooling operations over relatively large sets can also lead to over-squashing the signal. To help in these directions, we propose sampling  $X$  mini-batches of a certain size  $B$  at each iteration. At *step 1*, it samples  $B$  hyperedges from  $\mathcal{E}$ . The hyperedge sampling over  $\mathcal{E}$  can be either uniform or weighted (e.g. by taking into account hyperedge cardinalities). Then in *step 2*  $L$  nodes are in turn sampled from each sampled hyperedge  $e$ , padding the hyperedge with  $L - |e|$  special padding tokens if  $|e| > L$ . Overall, the shape of the obtained mini-batch  $X$  has fixed size  $B \times L$ . See Appendix H for additional analysis of the sampling procedure.

## 5 EXPERIMENTAL RESULTS

The questions that we introduced in the Introduction have shaped our research, leading to a new definition of higher-order homophily and novel architectural designs and sampling strategies that can potentially fit better the properties of hypergraph networks. In subsequent subsections, we set again three main questions that follow up from these fundamental inquiries and can help contextualize the technical contributions introduced in this paper.

**Dataset and Models** We use the same datasets used in Chien et al. (2022), which includes Cora, Citeseer, Pubmed, ModelNet40, NTU2012, 20Newsgroups, Mushroom, ZOO, CORA-CA, and DBLP-CA. More information about datasets and corresponding statistics can be found in Appendix F.2. We also utilize the benchmark implementation provided by Chien et al. (2022) to conduct the experiments with several models, including AllDeepSets, AllSetTransformer, UniGCNII, CEGAT, CEGCN, HCHA, HGNN, HNHN, HyperGCN, HAN, and HAN (mini-batching). Additionally, we consider vanilla MLP applied to node features and a transformer architecture and introduce three new models: MultiSetMixer, MLP Connectivity Batching (MLP CB), and Multiple MLP CB (MMLP CB). The MLP CB and MMLP CB models use connectivity information to form and process batches. Specifically, the MMLP CB model processes the top three most frequent connectivities using separate MLP encoders, while the fourth encoder is used to process the remaining connectivities. We refer to Section 4.3 for further details about all these architectures. All models are optimized using 15 splits with 2 model initializations, resulting in a total of 30 runs; see Appendix F.1 for further details.

## 5.1 HOW DOES MULTISETMIXER PERFORM?

Our first experiment aims to assess the performance of our proposed model, MultiSetMixer, as well as the two introduced baselines, MLP CB and MMLP CB. Figure 4 shows the average rankings –across all models and datasets– of the top-3 best performing models for the considered training splits, exhibiting that those splits can impact the relative performance among models.

However, due to space limitations, we restrict our analysis to the 50% split results shown in Table 1,<sup>1</sup> and relegate to Appendix G.1 the corresponding tables for the other scenarios. Table 1 emphasizes the MultiSetMixer model’s relatively solid performance, being the best-performing model on the NTU2012, ModelNet40, and 20NewsGroups datasets. Its performance on the 20NewsGroups dataset is especially noteworthy, significantly outperforming the other models. Moreover, it is notable that MLP CB and MMLP CB exhibit similar behaviour on this dataset. In contrast, the performance of all other models achieves roughly the same performance as the MLP. This observation suggests that these models can not account for dataset connectivity; in particular, as we demonstrated in Section 3, the dispersion of the node homophily measure, with a subsequent convergence to a similar value within each class, indicates that the dataset’s connectivity is notably non-homophilic and presents a challenge. In contrast, CORA-CA exhibits a high degree of homophily within its hyperedges and shows the most significant performance gap between the best-performing model, AllSetTransformer, and the basic MLP. A similar trend is observed for DBLP-CA (see node homophily plot in Appendix I). Please refer to Section 5.3 for additional experiments analyzing the impact of connectivity on the models.

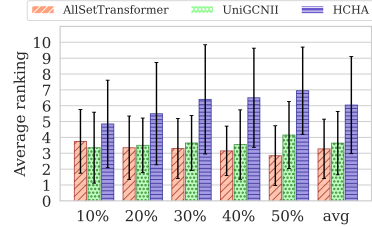


Figure 4: Average ranking and standard deviation for various training percentages.

Table 1: Hypergraph model performance benchmarks. Test accuracy in % averaged over 15 splits.

Model	Cora	Citeseer	Pubmed	CORA-CA	DBLP-CA	Mushroom	NTU2012	ModelNet40	20NewsGroups	ZOO	avg. ranking
AllDeepSets	77.11 ± 1.00	70.67 ± 1.42	<b>89.04 ± 0.45</b>	82.23 ± 1.46	91.34 ± 0.27	99.96 ± 0.05	86.49 ± 1.86	96.70 ± 0.25	81.19 ± 0.49	89.10 ± 7.00	6.00
AllSetTransformer	<b>79.54 ± 1.02</b>	72.52 ± 0.88	88.74 ± 0.51	<b>84.43 ± 1.14</b>	<b>91.61 ± 0.19</b>	99.95 ± 0.05	88.22 ± 1.42	<b>98.00 ± 0.12</b>	81.59 ± 0.59	<b>91.03 ± 7.31</b>	<b>2.85</b>
UniGCNII	78.46 ± 1.14	73.05 ± 1.48	88.07 ± 0.47	83.92 ± 1.02	91.56 ± 0.18	99.89 ± 0.07	88.24 ± 1.56	97.84 ± 0.16	81.16 ± 0.49	89.61 ± 8.09	4.15
CEGAT	76.53 ± 1.58	71.58 ± 1.11	87.11 ± 0.49	77.50 ± 1.51	88.74 ± 0.31	96.81 ± 1.41	82.27 ± 1.60	92.79 ± 0.44	OOM	44.62 ± 9.18	11.00
CEGCN	77.03 ± 1.31	70.87 ± 1.19	87.01 ± 0.62	77.55 ± 1.65	88.12 ± 0.25	94.91 ± 0.44	80.90 ± 1.74	90.04 ± 0.47	OOM	49.23 ± 6.81	11.67
HCHA	79.53 ± 1.33	72.57 ± 1.06	86.97 ± 0.55	83.53 ± 1.12	91.21 ± 0.28	98.94 ± 0.54	86.60 ± 1.96	94.50 ± 0.33	80.75 ± 0.53	89.23 ± 6.81	6.75
HGNN	79.53 ± 1.33	72.24 ± 1.08	86.97 ± 0.55	83.45 ± 1.22	91.26 ± 0.26	98.94 ± 0.54	86.71 ± 1.48	94.50 ± 0.33	80.75 ± 0.52	89.23 ± 6.81	6.85
HNHN	77.68 ± 1.08	73.47 ± 1.36	87.88 ± 0.47	78.53 ± 1.15	86.73 ± 0.40	<b>99.97 ± 0.04</b>	<b>88.28 ± 1.50</b>	97.84 ± 0.15	81.53 ± 0.55	89.23 ± 7.85	5.05
HyperGCN	74.78 ± 1.11	66.06 ± 1.58	82.32 ± 0.62	77.48 ± 1.14	86.07 ± 3.32	69.51 ± 4.98	47.65 ± 5.01	46.10 ± 7.95	80.84 ± 0.49	51.54 ± 9.88	13.80
HAN	<b>80.73 ± 1.37</b>	<b>73.69 ± 0.95</b>	86.34 ± 0.61	<b>84.19 ± 0.81</b>	91.10 ± 0.20	91.33 ± 0.91	83.78 ± 1.75	93.85 ± 0.33	79.67 ± 0.55	80.26 ± 6.42	8.10
HAN minibatch	80.24 ± 2.17	73.55 ± 1.13	85.41 ± 2.32	82.04 ± 2.56	90.52 ± 0.50	93.87 ± 1.04	80.62 ± 2.00	92.06 ± 0.63	79.76 ± 0.56	70.39 ± 11.29	9.90
MultiRepMixer	79.38 ± 1.08	72.79 ± 1.12	85.71 ± 0.49	82.62 ± 1.20	89.87 ± 0.29	95.85 ± 3.21	<b>88.73 ± 1.29</b>	<b>98.15 ± 0.19</b>	<b>87.83 ± 2.68</b>	78.67 ± 9.08	6.40
MLP CB	74.06 ± 1.26	71.93 ± 1.53	85.83 ± 0.51	74.39 ± 1.40	84.91 ± 0.44	96.83 ± 2.18	85.43 ± 1.51	96.41 ± 0.32	86.13 ± 2.82	81.61 ± 10.98	9.80
MMLP CB	71.05 ± 2.03	69.26 ± 1.91	85.20 ± 0.54	71.16 ± 2.17	84.08 ± 0.42	95.71 ± 2.42	NA	NA	85.04 ± 4.04	83.89 ± 9.52	12.75
MLP	73.27 ± 1.09	72.07 ± 1.65	87.13 ± 0.49	73.27 ± 1.09	84.77 ± 0.41	99.91 ± 0.08	79.70 ± 1.56	95.31 ± 0.28	80.93 ± 0.59	85.13 ± 6.90	10.40
Transformer	74.15 ± 1.17	71.82 ± 1.51	87.37 ± 0.49	73.61 ± 1.55	85.26 ± 0.38	99.95 ± 0.08	82.88 ± 1.93	96.29 ± 0.29	81.17 ± 0.54	88.72 ± 10.25	9.05

On the other hand, we can notice that CEGAT, CEGCN and our proposed model don’t perform well on the Mushroom dataset. This is noteworthy because the Mushroom dataset’s features are highly representative, as demonstrated by the near-perfect performance of the MLP classifier. This suggests that, in this particular case, connectivity may not play a crucial role in achieving high performance.

## 5.2 WHAT IS THE IMPACT OF THE INTRODUCED MINI-BATCH SAMPLING STRATEGY?

Next, we examine the role that our proposed mini-batching sampling can play (*i*) in explaining previous results and (*ii*) in influencing other model’s performance.

**Class distribution analysis** To evaluate and motivate the potential of the proposed mini-batching sampling, we investigate the reason behind both the superior performance of MultiSetMixer, MLP CB and MMLP CB on 20NewsGroup and their poor performance on Mushroom. Framing mini-batching from the connectivity perspective presents a nuanced challenge that conceals significant potential for improvement (Teney et al., 2023). It is important to note that connectivity, by definition,

<sup>1</sup>Unless otherwise specified, all tables in the main body of the paper use a 50%/25%/25% split between training and testing. The results are shown as Mean Accuracy Standard Deviation, with the best result highlighted in bold and shaded in grey, and results within one standard deviation of the best result are displayed in blue-shaded boxes.

describes relationships among the nodes, implying that some parts of the dataset might interconnect much more densely, creating some sort of hubs within the network. Thus, mini-batching might introduce unexpected skew in training distribution. In particular, in Figure 5, we depict the class distribution of the original dataset, referred to as *Node*, while ‘*Step 1 and 2*’ and ‘*Step 1*’ shows the distribution after each step in our mini-batching procedure. The sampling procedure tends to rebalance class distributions in certain cases, such as the 20NewsGroup dataset, while in contrast, it introduces an imbalance that was not present in the original labels in the Mushroom dataset, where our model demonstrated suboptimal performance. This observation leads to the hypothesis that, in some cases, the sampling procedure produces a shift distribution that rebalances the class distributions and conducts our model to outperform the comparison models.

**Application to Other Models** Furthermore, we explore the proposed mini-batch sampling procedure with the AllSetTransformer and UniGCNII models by implementing Step 1 of the mini-batch procedure without additional hyperparameter optimization. From Table 2, we can observe a drop in performance for most of the datasets both for AllSetTransformer and for UniGCNII; both models, on average, outperform the HAN (mini-batching) model. This suggests the substantial potential of the proposed sampling procedure. More in detail, AllsetTransformer has a substantial decrease in accuracy for the CORA-CA dataset, in contrast to the UniGCNII, which registers only marginal decreases. A parallel pattern emerges with the DBLP-CA dataset.

Table 2: Mini-batching experiment. Test accuracy in % averaged over 15 splits

Model	Cora	Citeseer	Pubmed	CORA-CA	DBLP-CA	Mushroom	NTU2012	ModelNet40	20Newsgroups	ZOO	avg. ranking
AllSetTransformer (batched)	74.34 ± 1.08	69.67 ± 1.46	87.75 ± 0.30	75.75 ± 1.46	86.06 ± 0.22	99.91 ± 0.05	87.55 ± 0.86	96.42 ± 0.17	81.37 ± 0.28	93.20 ± 5.38	2.70
UniGCNII (batched)	77.88 ± 0.69	69.51 ± 0.87	86.82 ± 0.33	83.12 ± 0.89	90.45 ± 0.28	99.95 ± 0.04	87.64 ± 0.99	97.55 ± 0.17	81.23 ± 0.31	90.00 ± 4.43	2.20
HAN minibatch	80.24 ± 2.17	73.55 ± 1.13	85.41 ± 2.32	82.04 ± 2.56	90.52 ± 0.50	93.87 ± 1.04	80.62 ± 2.00	92.06 ± 0.63	79.76 ± 0.56	70.39 ± 11.29	3.00
MultiSetMixer	79.38 ± 1.08	72.79 ± 1.12	85.71 ± 0.49	82.62 ± 1.20	89.87 ± 0.29	95.85 ± 3.21	88.73 ± 1.29	98.15 ± 0.19	87.83 ± 2.68	78.67 ± 9.08	2.10

### 5.3 HOW DO CONNECTIVITY CHANGES AFFECT PERFORMANCE?

To shine a light on this, we design two different experimental approaches aiming at modifying the original connectivity of datasets in a systematic manner. The first experiment tests the performance when some hyperedges are removed following different *drop connectivity* strategies. Then, a second experiment examines the model’s performance with the introduction of two preprocessing strategies applied to the given hypergraph connectivity.

**Reducing Connectivity** This experiment aims to investigate the significance of connectivity in datasets and the extent to which it influences the performances of the models. We divide this experiment into two parts: (i) drop connectivity and (ii) connectivity rewiring. In the first part of the experiment, we employ three strategies to introduce variations in the initial dataset’s connectivity. The first two strategies involve ordering hyperedges based on their lengths in **ascending order**. In the first approach, referred to as *trimming*, we remove the initial  $x\%$  of ordered hyperedges. The second approach, referred to as *retention*, involves keeping the first  $x\%$  of hyperedges and discarding the remaining  $100 - x\%$ . Finally, the last strategy involves randomly dropping  $x\%$  of hyperedges from the dataset, referred to as *random drop*. Results shown in Table 3 also indicate that connectivity minimally impacts CEGCN, and AllSetTransformer for the Citeseer and Pubmed datasets. On the other hand, MultiSetMixer performs better at the *trimming 25%* setting, although the achieved performance is on par with MLP reported in Table 1. This suggests that the proposed model was negatively affected by the distribution shift. Conversely, we observe a similar but opposite trend for the Mushroom dataset, where MultiSetMixer’s performance improves due to the reduced impact of the distribution shift. Another interesting observation is that the CEGCN model gains improvement in 6 out of 9 datasets, with a doubled increase for the ZOO dataset. In the case of Cora, CORA-CA, and DBLP-CA datasets, another interesting pattern emerges: retaining only 25% of the highest relationships (*retention 25%*) consistently results in better performance compared to retaining 50% or 75%. This is intriguing because, at the 25% level, we are preserving only a small fraction of the higher-order relationships. The opposite pattern holds for the *trimming* strategy. For the

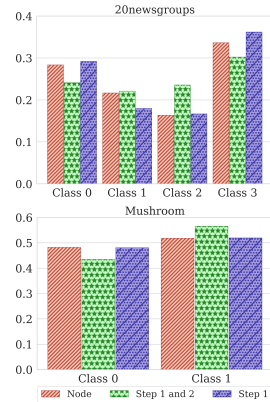


Figure 5: Distribution of classes

datasets mentioned above, this phenomenon remained consistent across all models. Notice that this phenomenon doesn't appear when we remove hyperedges randomly, in this case, as expected, the more hyperedges we remove, the more the performances decrease.

**Rewiring Connectivity** In this experiment, we preserve the original connectivity and investigate the influence of homophilic hyperedges on performance. To do so, we adjust the given connectivity in two different ways. The first strategy aims to unveil the full potential of homophily for each dataset by dividing the given hyperedges into fully homophilic ones based on the *node labels*. In contrast, the second strategy explores the possibility of splitting hyperedges based on their *initial node features*. More in detail, the hyperedge division results from applying multiple times *k*-means for each hyperedge *e*, varying at each iteration the number of centroids *m* from 2 to  $\min(C, |e|)$ ; the elbow method is then used to determine the optimal hyperedge partitioning. It's not surprising that the "Label Based" strategy improves the performance for all datasets and models, as evident from Table 4. However, it's worth highlighting that the graph-based method CEGCN achieves results similar to HGNNs in this strategy. Additionally, only CEGCN, on average, performs better with the "k-means" strategy. These observations collectively suggest that connectivity preprocessing plays a crucial role, particularly for graph-based models. Applying "k-means" diminishes the distribution shift for MultiSetMixer.

Table 3: Drop connectivity benchmarks. Test accuracy in % averaged over 15 splits.

Model	Type	Cora	Citeseer	Pubmed	CORA-CA	DBLP-CA	Mushroom	NTU2012	ModelNet40	20NewsGroups	ZOO	avg. ranking
AllSetTransformer	Original	<b>79.54 ± 1.02</b>	72.52 ± 0.88	<b>88.74 ± 0.51</b>	<b>84.43 ± 1.14</b>	<b>91.61 ± 0.19</b>	99.95 ± 0.05	<b>88.22 ± 1.42</b>	<b>98.00 ± 0.12</b>	81.59 ± 0.59	91.03 ± 7.31	<b>1.95</b>
	Random 25%	79.11 ± 0.99	<b>72.75 ± 1.14</b>	88.67 ± 0.47	82.36 ± 1.38	90.61 ± 0.29	99.94 ± 0.09	87.50 ± 1.36	97.98 ± 0.17	<b>81.70 ± 0.52</b>	89.87 ± 7.66	3.10
	Random 50%	77.77 ± 1.34	72.21 ± 1.25	88.50 ± 0.45	79.73 ± 1.58	89.46 ± 0.27	99.96 ± 0.04	87.34 ± 1.55	97.83 ± 0.17	81.55 ± 0.66	89.49 ± 6.30	5.85
	Random 75%	76.92 ± 1.20	72.40 ± 1.22	88.54 ± 0.47	77.88 ± 1.74	87.73 ± 0.32	99.76 ± 0.15	86.31 ± 1.34	97.52 ± 0.20	81.46 ± 0.62	87.69 ± 6.09	8.10
	Retention 25%	<b>79.19 ± 1.11</b>	72.49 ± 0.86	88.73 ± 0.40	<b>83.58 ± 1.30</b>	91.18 ± 0.17	<b>99.93 ± 0.09</b>	<b>87.21 ± 1.58</b>	97.82 ± 0.17	81.63 ± 0.48	86.92 ± 7.18	4.10
	Retention 50%	78.16 ± 0.98	72.55 ± 1.13	88.70 ± 0.37	82.90 ± 1.15	90.80 ± 0.22	99.89 ± 0.18	86.67 ± 1.64	97.36 ± 0.21	81.61 ± 0.49	88.08 ± 7.51	5.20
	Retention 75%	77.38 ± 1.35	72.43 ± 0.98	88.71 ± 0.39	81.07 ± 1.20	89.83 ± 0.25	<b>99.97 ± 0.04</b>	85.58 ± 1.70	97.27 ± 0.22	81.58 ± 0.48	88.97 ± 6.91	5.80
	Trimming 25%	75.83 ± 1.31	72.39 ± 1.50	88.40 ± 0.45	76.51 ± 1.35	86.38 ± 0.32	99.84 ± 0.13	<b>86.88 ± 1.66</b>	97.10 ± 0.24	81.55 ± 0.55	<b>93.08 ± 7.79</b>	8.05
	Trimming 50%	77.37 ± 1.17	72.32 ± 1.30	88.49 ± 0.40	77.41 ± 1.73	87.03 ± 0.27	99.91 ± 0.12	86.86 ± 1.53	97.86 ± 0.21	81.45 ± 0.50	89.74 ± 8.53	7.50
	Trimming 75%	78.15 ± 1.11	72.67 ± 1.00	88.48 ± 0.39	78.91 ± 1.54	88.55 ± 0.26	99.92 ± 0.09	87.68 ± 1.56	97.90 ± 0.23	81.41 ± 0.61	91.03 ± 7.17	5.35
CEGCN	Original	<b>77.03 ± 1.31</b>	70.87 ± 1.19	87.01 ± 0.62	<b>77.55 ± 1.65</b>	<b>88.12 ± 0.25</b>	94.91 ± 0.44	80.90 ± 1.74	90.04 ± 0.47	OOM	49.23 ± 6.81	4.61
	Random 25%	<b>76.08 ± 1.55</b>	71.35 ± 1.44	86.89 ± 0.59	<b>76.51 ± 1.53</b>	87.01 ± 0.39	93.11 ± 0.46	80.68 ± 1.86	90.36 ± 0.46	OOM	49.74 ± 6.22	6.22
	Random 50%	75.55 ± 1.63	71.42 ± 1.60	86.70 ± 0.48	75.27 ± 1.22	86.24 ± 0.35	93.28 ± 0.61	80.63 ± 1.78	90.69 ± 0.54	OOM	56.92 ± 7.24	6.33
	Random 75%	75.34 ± 1.62	71.73 ± 1.90	<b>86.97 ± 0.51</b>	74.53 ± 1.56	85.36 ± 0.26	93.01 ± 0.45	80.56 ± 1.76	<b>91.91 ± 0.54</b>	OOM	63.20 ± 5.59	6.33
	Retention 25%	<b>76.12 ± 1.58</b>	70.87 ± 1.42	86.94 ± 0.56	<b>76.98 ± 1.53</b>	<b>87.90 ± 0.29</b>	94.94 ± 0.48	79.20 ± 1.42	90.59 ± 0.59	OOM	49.87 ± 7.59	5.50
	Retention 50%	75.43 ± 1.28	70.83 ± 1.52	86.95 ± 0.54	76.87 ± 1.49	87.58 ± 0.28	94.97 ± 0.40	78.53 ± 1.90	90.09 ± 0.56	OOM	45.77 ± 6.88	6.89
	Retention 75%	75.53 ± 1.25	71.72 ± 1.42	87.11 ± 0.53	76.36 ± 1.42	87.03 ± 0.28	94.74 ± 0.39	79.82 ± 1.41	<b>92.29 ± 0.46</b>	OOM	40.38 ± 5.42	5.44
	Trimming 25%	75.58 ± 1.56	<b>72.26 ± 1.52</b>	<b>87.36 ± 0.51</b>	74.84 ± 1.31	84.97 ± 0.31	<b>99.60 ± 0.11</b>	<b>83.10 ± 1.69</b>	<b>91.85 ± 0.42</b>	OOM	<b>87.69 ± 7.31</b>	<b>3.44</b>
	Trimming 50%	<b>76.57 ± 1.47</b>	71.81 ± 1.44	87.07 ± 0.55	74.66 ± 1.68	85.24 ± 0.33	<b>99.54 ± 0.18</b>	80.72 ± 1.64	90.64 ± 0.54	OOM	71.28 ± 6.60	4.00
	Trimming 75%	<b>76.53 ± 1.50</b>	71.45 ± 1.45	86.75 ± 0.54	74.56 ± 1.32	85.56 ± 0.33	99.14 ± 0.23	80.38 ± 1.91	90.06 ± 0.37	OOM	58.46 ± 7.17	6.22
MultiSetMixer	Original	<b>79.38 ± 1.08</b>	<b>72.79 ± 1.12</b>	85.71 ± 0.49	<b>82.62 ± 1.20</b>	<b>89.87 ± 0.29</b>	95.85 ± 3.21	<b>88.73 ± 1.29</b>	<b>98.15 ± 0.19</b>	<b>87.83 ± 2.68</b>	<b>78.67 ± 9.08</b>	<b>2.75</b>
	Random 25%	<b>78.63 ± 1.30</b>	72.37 ± 1.50	85.71 ± 0.55	81.18 ± 1.16	89.11 ± 0.31	93.80 ± 4.69	<b>87.92 ± 1.50</b>	<b>98.01 ± 0.19</b>	76.65 ± 1.76	77.60 ± 9.00	4.75
	Random 50%	77.66 ± 1.18	72.24 ± 1.42	85.92 ± 0.45	78.51 ± 1.58	88.13 ± 0.34	94.36 ± 3.79	86.22 ± 2.01	97.92 ± 0.13	74.36 ± 1.23	75.53 ± 14.10	6.40
	Random 75%	<b>76.59 ± 1.27</b>	72.12 ± 1.43	86.10 ± 0.53	76.91 ± 1.43	86.42 ± 0.42	98.74 ± 0.90	85.31 ± 1.64	97.48 ± 0.21	76.53 ± 1.25	58.75 ± 17.97	7.25
	Retention 25%	<b>78.99 ± 1.00</b>	72.12 ± 1.28	85.73 ± 0.44	<b>82.01 ± 1.56</b>	<b>89.61 ± 0.33</b>	97.18 ± 2.01	86.96 ± 1.62	97.95 ± 0.19	<b>88.17 ± 2.51</b>	<b>80.15 ± 8.87</b>	3.85
	Retention 50%	77.88 ± 1.28	72.32 ± 1.36	85.89 ± 0.52	80.85 ± 1.14	89.24 ± 0.31	97.72 ± 1.42	84.56 ± 1.97	97.39 ± 0.24	85.04 ± 2.06	76.31 ± 12.45	5.20
	Retention 75%	77.44 ± 1.32	72.18 ± 1.32	85.93 ± 0.54	78.67 ± 1.32	87.86 ± 0.35	94.75 ± 3.86	83.94 ± 1.79	97.00 ± 0.26	84.65 ± 1.52	67.06 ± 18.55	7.10
	Trimming 25%	75.54 ± 1.17	72.57 ± 1.45	<b>87.26 ± 0.38</b>	76.30 ± 1.11	85.57 ± 0.34	<b>99.97 ± 0.03</b>	83.19 ± 1.55	96.87 ± 0.29	78.80 ± 0.52	<b>88.51 ± 9.76</b>	6.00
	Trimming 50%	76.91 ± 1.18	72.30 ± 1.63	86.79 ± 0.53	77.54 ± 1.44	86.16 ± 0.33	99.91 ± 0.13	84.20 ± 1.75	97.70 ± 0.27	72.70 ± 0.88	69.83 ± 14.25	6.60
	Trimming 75%	78.06 ± 1.16	<b>72.53 ± 1.30</b>	86.45 ± 0.57	79.03 ± 1.16	87.83 ± 0.29	98.49 ± 0.61	86.59 ± 1.58	97.86 ± 0.24	61.17 ± 1.32	76.08 ± 10.14	5.10

Table 4: Adjust connectivity. Test accuracy in % averaged over 15 splits.

Model	Type	Cora	Citeseer	Pubmed	CORA-CA	DBLP-CA	Mushroom	NTU2012	ModelNet40	20NewsGroups	ZOO	avg. ranking
AllDeepSets	Label Based	<b>82.24 ± 1.12</b>	<b>75.65 ± 1.57</b>	<b>90.49 ± 0.40</b>	<b>91.12 ± 0.92</b>	<b>96.59 ± 0.17</b>	<b>99.96 ± 0.04</b>	<b>93.13 ± 1.29</b>	<b>99.52 ± 0.11</b>	<b>99.79 ± 0.13</b>	<b>91.54 ± 7.24</b>	<b>1.05</b>
	k-means	75.20 ± 1.11	70.87 ± 1.54	88.96 ± 0.48	79.59 ± 1.42	89.75 ± 0.25	99.94 ± 0.09	84.23 ± 1.50	97.17 ± 0.13	81.18 ± 0.54	86.92 ± 7.73	2.80
	Original	77.11 ± 1.00	70.67 ± 1.42	89.04 ± 0.45	82.23 ± 1.46	91.34 ± 0.27	<b>99.96 ± 0.05</b>	86.49 ± 1.86	96.70 ± 0.25	81.19 ± 0.49	89.10 ± 7.00	2.15
AllSetTransformer	Label Based	<b>83.43 ± 1.36</b>	<b>76.45 ± 1.43</b>	<b>90.19 ± 0.42</b>	<b>91.71 ± 0.89</b>	<b>96.75 ± 0.16</b>	<b>99.96 ± 0.05</b>	<b>94.81 ± 1.04</b>	<b>99.68 ± 0.09</b>	<b>99.93 ± 0.03</b>	<b>94.10 ± 6.91</b>	<b>1.05</b>
	k-means	77.14 ± 1.46	72.83 ± 1.07	88.60 ± 0.41	81.92 ± 1.35	89.79 ± 0.30	<b>99.96 ± 0.06</b>	87.95 ± 1.28	97.29 ± 0.20	81.58 ± 0.55	88.72 ± 7.69	2.75
	Original	79.54 ± 1.02	72.52 ± 0.88	88.74 ± 0.51	84.43 ± 1.14	91.61 ± 0.19	99.95 ± 0.05	88.22 ± 1.42	98.00 ± 0.12	81.59 ± 0.59	91.03 ± 7.31	2.20
CEGCN	Label Based	<b>83.70 ± 1.02</b>	<b>77.50 ± 1.53</b>	<b>90.08 ± 0.42</b>	<b>91.28 ± 0.97</b>	<b>96.68 ± 0.14</b>	<b>99.95 ± 0.05</b>	<b>94.03 ± 1.24</b>	<b>99.30 ± 0.14</b>	OOM	<b>95.00 ± 7.08</b>	<b>1.00</b>
	k-means	75.89 ± 1.53	72.07 ± 1.18	87.13 ± 0.51	76.43 ± 1.41	86.76 ± 0.24	94.84 ± 0.47	85.34 ± 1.71	95.77 ± 0.31	OOM	73.72 ± 7.89	2.44
	Original	77.03 ± 1.31	70.87 ± 1.19	87.01 ± 0.62	77.55 ± 1.65	88.12 ± 0.25	94.91 ± 0.44	80.90 ± 1.74	90.04 ± 0.47	OOM	49.23 ± 6.81	2.56
MultiSetMixer	Label Based	<b>82.59 ± 0.94</b>	<b>76.14 ± 1.03</b>	<b>88.35 ± 0.59</b>	<b>90.86 ± 0.67</b>	<b>96.38 ± 0.22</b>	<b>99.97 ± 0.04</b>	<b>93.72 ± 1.00</b>	<b>99.56 ± 0.12</b>	<b>99.85 ± 0.06</b>	<b>91.79 ± 6.90</b>	<b>1.05</b>
	k-means based	76.78 ± 1.15	73.10 ± 1.18	85.84 ± 0.59	80.06 ± 1.45	88.54 ± 0.27	<b>99.97 ± 0.05</b>	87.75 ± 1.09	96.94 ± 0.26	81.14 ± 0.47	<b>85.41 ± 6.77</b>	2.55
	Original	79.38 ± 1.08	72.79 ± 1.12	85.71 ± 0.49	82.62 ± 1.20	89.87 ± 0.29	95.85 ± 3.21	88.73 ± 1.29	98.15 ± 0.19	87.83 ± 2.68	78.67 ± 9.08	2.40

## 6 DISCUSSION

This section summarizes some key findings from our extensive evaluation and proposed homophily measure. Firstly, we showed that the proposed message passing formalization of the homophily measure enables the discovery of patterns and provides valuable insights into the dynamics of hypernetworks. Importantly, this approach can be extended to other definitions of homophily beyond labels. Furthermore, we showed that our MultiSetMixer model outperforms existing architectures in several scenarios. We also identified some common failure modes, which we attribute to the distribution shift introduced by the proposed mini-batching sampling scheme and the way message-passing propagates information. The experimental results demonstrate that certain benchmark datasets (Citeseer, Pubmed, 20NewsGroups) for hypergraph learning contain connectivity patterns that are not

---

effectively captured by HGNNs and are often overlooked. We show that the substantial performance gap between HGNNs and MLP for Cora, CORA-CA, and DBLP-CA is primarily attributed to patterns within a particular subset of connectivity, i.e., the largest hyperedge cardinalities have a stronger influence on performance. Finally, there is compelling evidence that connectivity can serve purposes beyond message propagation, such as acting as a tool for intentional distribution shift with mini-batching. We believe that the provided set of experiments and dynamic homophily figures are valuable tools to shape novel ideas for the hypergraph modeling research field.

## 7 REPRODUCIBILITY

We include all the details about our experimental setting, including the choice of hyperparameters, the specifications of our machine and environment, the training/validation/test split, in Appendix F.1 and in Section 5. To ensure the reproducibility of our results, we will provide the source code along with the camera-ready version.

## REFERENCES

- Sameer Agarwal, Kristin Branson, and Serge Belongie. Higher order learning with graphs. In *Proceedings of the 23rd international conference on Machine learning*, pp. 17–24, 2006.
- Devanshu Arya, Deepak K Gupta, Stevan Rudinac, and Marcel Worring. Hypersage: Generalizing inductive representation learning on hypergraphs. *arXiv preprint arXiv:2010.04558*, 2020.
- Jimmy Lei Ba, Jamie Ryan Kiros, and Geoffrey E Hinton. Layer normalization. *arXiv preprint arXiv:1607.06450*, 2016.
- Song Bai, Feihu Zhang, and Philip HS Torr. Hypergraph convolution and hypergraph attention. *Pattern Recognition*, 110:107637, 2021.
- Muhammet Balcilar, Pierre Héroux, Benoit Gauzere, Pascal Vasseur, Sébastien Adam, and Paul Honeine. Breaking the limits of message passing graph neural networks. In *International Conference on Machine Learning*, pp. 599–608. PMLR, 2021.
- Ding-Yun Chen, Xiao-Pei Tian, Yu-Te Shen, and Ming Ouhyoung. On visual similarity based 3d model retrieval. In *Computer graphics forum*, volume 22, pp. 223–232. Wiley Online Library, 2003.
- Guanzi Chen and Jiying Zhang. Preventing over-smoothing for hypergraph neural networks. *arXiv preprint arXiv:2203.17159*, 2022.
- Ming Chen, Zhewei Wei, Zengfeng Huang, Bolin Ding, and Yaliang Li. Simple and deep graph convolutional networks. In *International conference on machine learning*, pp. 1725–1735. PMLR, 2020.
- Eli Chien, Jianhao Peng, Pan Li, and Olgica Milenkovic. Adaptive universal generalized pagerank graph neural network. *arXiv preprint arXiv:2006.07988*, 2020.
- Eli Chien, Chao Pan, Jianhao Peng, and Olgica Milenkovic. You are allset: A multiset function framework for hypergraph neural networks. In *International Conference on Learning Representations*, 2022. URL [https://openreview.net/forum?id=hpBTIv2uy\\_E](https://openreview.net/forum?id=hpBTIv2uy_E).
- Yihe Dong, Will Sawin, and Yoshua Bengio. Hnhn: Hypergraph networks with hyperedge neurons. *arXiv preprint arXiv:2006.12278*, 2020.
- Dheeru Dua, Casey Graff, et al. Uci machine learning repository, 2017. URL <http://archive.ics.uci.edu/ml>, 7(1), 2017.
- Yifan Feng, Haoxuan You, Zizhao Zhang, Rongrong Ji, and Yue Gao. Hypergraph neural networks. In *Proceedings of the AAAI conference on artificial intelligence*, volume 33, pp. 3558–3565, 2019.
- Yue Gao, Meng Wang, Dacheng Tao, Rongrong Ji, and Qionghai Dai. 3-d object retrieval and recognition with hypergraph analysis. *IEEE transactions on image processing*, 21(9):4290–4303, 2012.

- 
- Fangda Gu, Heng Chang, Wenwu Zhu, Somayeh Sojoudi, and Laurent El Ghaoui. Implicit graph neural networks. *Advances in Neural Information Processing Systems*, 33:11984–11995, 2020.
- Jonathan Halcrow, Alexandru Mosoi, Sam Ruth, and Bryan Perozzi. Grale: Designing networks for graph learning. In *Proceedings of the 26th ACM SIGKDD international conference on knowledge discovery & data mining*, pp. 2523–2532, 2020.
- Matthias Hein, Simon Setzer, Leonardo Jost, and Syama Sundar Rangapuram. The total variation on hypergraphs-learning on hypergraphs revisited. *Advances in Neural Information Processing Systems*, 26, 2013.
- Jing Huang and Jie Yang. Unignn: a unified framework for graph and hypergraph neural networks. In Zhi-Hua Zhou (ed.), *Proceedings of the Thirtieth International Joint Conference on Artificial Intelligence, IJCAI-21*, pp. 2563–2569. International Joint Conferences on Artificial Intelligence Organization, 8 2021. doi: 10.24963/ijcai.2021/353. URL <https://doi.org/10.24963/ijcai.2021/353>. Main Track.
- Sungwoong Kim, Sebastian Nowozin, Pushmeet Kohli, and Chang Yoo. Higher-order correlation clustering for image segmentation. *Advances in neural information processing systems*, 24, 2011.
- Thomas N Kipf and Max Welling. Semi-supervised classification with graph convolutional networks. In *International Conference on Learning Representations*, 2017.
- Steffen Klamt, Utz-Uwe Haus, and Fabian Theis. Hypergraphs and cellular networks. *PLoS computational biology*, 5(5):e1000385, 2009.
- Valerio La Gatta, Vincenzo Moscato, Mirko Pennone, Marco Postiglione, and Giancarlo Sperlì. Music recommendation via hypergraph embedding. *IEEE Transactions on Neural Networks and Learning Systems*, 2022.
- Juho Lee, Yoonho Lee, Jungtaek Kim, Adam Kosiosek, Seungjin Choi, and Yee Whye Teh. Set transformer: A framework for attention-based permutation-invariant neural networks. In *International conference on machine learning*, pp. 3744–3753. PMLR, 2019.
- Jiachen Li, Chuanbo Hua, Jinkyoo Park, Hengbo Ma, Victoria Dax, and Mykel J Kochenderfer. Evolvehypergraph: Group-aware dynamic relational reasoning for trajectory prediction. *arXiv preprint arXiv:2208.05470*, 2022a.
- Mengran Li, Yong Zhang, Xiaoyong Li, Yuchen Zhang, and Baocai Yin. Hypergraph transformer neural networks. *ACM Transactions on Knowledge Discovery from Data (TKDD)*, 2022b.
- Pan Li and Olgica Milenkovic. Inhomogeneous hypergraph clustering with applications. *Advances in neural information processing systems*, 30, 2017.
- James Moody. Race, school integration, and friendship segregation in america. *American journal of Sociology*, 107(3):679–716, 2001.
- Wesley Shrum, Neil H Cheek Jr, and Sandra MacD. Friendship in school: Gender and racial homophily. *Sociology of Education*, pp. 227–239, 1988.
- Hang Su, Subhransu Maji, Evangelos Kalogerakis, and Erik Learned-Miller. Multi-view convolutional neural networks for 3d shape recognition. In *Proceedings of the IEEE international conference on computer vision*, pp. 945–953, 2015.
- Damien Teney, Jindong Wang, and Ehsan Abbasnejad. Selective mixup helps with distribution shifts, but not (only) because of mixup. *arXiv preprint arXiv:2305.16817*, 2023.
- Ilya O Tolstikhin, Neil Houlsby, Alexander Kolesnikov, Lucas Beyer, Xiaohua Zhai, Thomas Unterthiner, Jessica Yung, Andreas Steiner, Daniel Keysers, Jakob Uszkoreit, et al. Mlp-mixer: An all-mlp architecture for vision. *Advances in neural information processing systems*, 34:24261–24272, 2021.
- Ashish Vaswani, Noam Shazeer, Niki Parmar, Jakob Uszkoreit, Llion Jones, Aidan N Gomez, Łukasz Kaiser, and Illia Polosukhin. Attention is all you need. *Advances in neural information processing systems*, 30, 2017.

- 
- Nate Veldt, Austin R Benson, and Jon Kleinberg. Combinatorial characterizations and impossibilities for higher-order homophily. *Science Advances*, 9(1):eabq3200, 2023.
- Petar Veličković, Guillem Cucurull, Arantxa Casanova, Adriana Romero, Pietro Lio, and Yoshua Bengio. Graph attention networks. *arXiv preprint arXiv:1710.10903*, 2017.
- Lois M Verbrugge. A research note on adult friendship contact: a dyadic perspective. *Soc. F.*, 62:78, 1983.
- Peihao Wang, Shenghao Yang, Yunyu Liu, Zhangyang Wang, and Pan Li. Equivariant hypergraph diffusion neural operators. In *The Eleventh International Conference on Learning Representations*, 2023. URL <https://openreview.net/forum?id=RiTjKoscnNd>.
- Xiao Wang, Houye Ji, Chuan Shi, Bai Wang, Yanfang Ye, Peng Cui, and Philip S Yu. Heterogeneous graph attention network. In *The world wide web conference*, pp. 2022–2032, 2019.
- Jinfeng Wei, Yunxin Wang, Mengli Guo, Pei Lv, Xiaoshan Yang, and Mingliang Xu. Dynamic hypergraph convolutional networks for skeleton-based action recognition. *arXiv preprint arXiv:2112.10570*, 2021.
- Zhirong Wu, Shuran Song, Aditya Khosla, Fisher Yu, Linguang Zhang, Xiaoou Tang, and Jianxiong Xiao. 3d shapenets: A deep representation for volumetric shapes. In *Proceedings of the IEEE conference on computer vision and pattern recognition*, pp. 1912–1920, 2015.
- Chenxin Xu, Maosen Li, Zhenyang Ni, Ya Zhang, and Siheng Chen. Groupnet: Multiscale hypergraph neural networks for trajectory prediction with relational reasoning. In *Proceedings of the IEEE/CVF Conference on Computer Vision and Pattern Recognition*, pp. 6498–6507, 2022.
- Naganand Yadati. Neural message passing for multi-relational ordered and recursive hypergraphs. In H. Larochelle, M. Ranzato, R. Hadsell, M.F. Balcan, and H. Lin (eds.), *Advances in Neural Information Processing Systems*, volume 33, pp. 3275–3289. Curran Associates, Inc., 2020. URL [https://proceedings.neurips.cc/paper\\_files/paper/2020/file/217eedd1ba8c592db97d0dbe54c7adfc-Paper.pdf](https://proceedings.neurips.cc/paper_files/paper/2020/file/217eedd1ba8c592db97d0dbe54c7adfc-Paper.pdf).
- Naganand Yadati, Madhav Nimishakavi, Prateek Yadav, Vikram Nitin, Anand Louis, and Partha Talukdar. HypergcN: A new method for training graph convolutional networks on hypergraphs. *Advances in neural information processing systems*, 32, 2019.
- Naganand Yadati, Vikram Nitin, Madhav Nimishakavi, Prateek Yadav, Anand Louis, and Partha Talukdar. Nhp: Neural hypergraph link prediction. In *Proceedings of the 29th ACM International Conference on Information & Knowledge Management, CIKM '20*, pp. 1705–1714, New York, NY, USA, 2020. Association for Computing Machinery. ISBN 9781450368599. doi: 10.1145/3340531.3411870. URL <https://doi.org/10.1145/3340531.3411870>.
- Chaoqi Yang, Ruijie Wang, Shuochao Yao, and Tarek Abdelzaher. Hypergraph learning with line expansion. *arXiv preprint arXiv:2005.04843*, 2020.
- Jaehyuk Yi and Jinkyoo Park. Hypergraph convolutional recurrent neural network. In *Proceedings of the 26th ACM SIGKDD international conference on knowledge discovery & data mining*, pp. 3366–3376, 2020.
- Hao Yin, Austin R Benson, Jure Leskovec, and David F Gleich. Local higher-order graph clustering. In *Proceedings of the 23rd ACM SIGKDD international conference on knowledge discovery and data mining*, pp. 555–564, 2017.
- Junliang Yu, Hongzhi Yin, Jundong Li, Qinyong Wang, Nguyen Quoc Viet Hung, and Xiangliang Zhang. Self-supervised multi-channel hypergraph convolutional network for social recommendation. In *Proceedings of the web conference 2021*, pp. 413–424, 2021.
- Manzil Zaheer, Satwik Kottur, Siamak Ravanbakhsh, Barnabas Poczos, Russ R Salakhutdinov, and Alexander J Smola. Deep sets. *Advances in neural information processing systems*, 30, 2017.

- 
- Muhan Zhang, Zhicheng Cui, Shali Jiang, and Yixin Chen. Beyond link prediction: Predicting hyperlinks in adjacency space. In *Proceedings of the AAAI Conference on Artificial Intelligence*, volume 32, 2018.
- Xiaoyao Zheng, Yonglong Luo, Liping Sun, Xintao Ding, and Ji Zhang. A novel social network hybrid recommender system based on hypergraph topologic structure. *World Wide Web*, 21: 985–1013, 2018.
- Dengyong Zhou, Jiayuan Huang, and Bernhard Schölkopf. Learning with hypergraphs: Clustering, classification, and embedding. *Advances in neural information processing systems*, 19, 2006.
- Jie Zhou, Ganqu Cui, Shengding Hu, Zhengyan Zhang, Cheng Yang, Zhiyuan Liu, Lifeng Wang, Changcheng Li, and Maosong Sun. Graph neural networks: A review of methods and applications. *AI open*, 1:57–81, 2020.

---

# Supplementary Materials

## A EXTENDED RELATED WORKS ON HYPERGRAPH NEURAL NETWORKS

Numerous machine-learning techniques have been developed for processing hypergraph data. One commonly used approach in early literature is to transform the hypergraph into a graph through clique expansion (CE). This technique involves substituting each hyperedge with an edge for every pair of vertices within the hyperedge, creating a graph that can be analyzed using graph-based algorithms (Agarwal et al., 2006; Zhou et al., 2006; Zhang et al., 2018; Li & Milenkovic, 2017).

Several techniques have been proposed that use Hypergraph Neural Networks (HGNNs) for semi-supervised learning. One of the earliest methods extends the graph convolution operator by incorporating the normalized hypergraph Laplacian (Feng et al., 2019). As pointed out in Dong et al. (2020), spectral convolution with the normalized Laplacian corresponds to performing a weighted CE of the hypergraph. HyperGCN (Yadati et al., 2019) employs mediators for incomplete CE on the hypergraph, which reduces the number of edges required to represent a hyperedge from a quadratic to a linear number of edges. The information diffusion is then carried out using spectral convolution for hypergraph-based semi-supervised learning. Hypergraph Convolution and Hypergraph Attention (HCHA) (Bai et al., 2021) employs modified degree normalizations and attention weights, with the attention weights depending on node and hyperedge features.

CE may cause the loss of important structural information and result in suboptimal learning performance (Hein et al., 2013; Chien et al., 2022). Furthermore, these models typically obtain the best performance with shallow 2-layer architectures. Adding more layers can lead to reduced performance due to oversmoothing (Huang & Yang, 2021). In the recent study Chen & Zhang (2022), an attempt was made to address oversmoothing in this type of network by incorporating residual connections; however, the method still relies on using hypergraph Laplacians to build a weighted graph through clique expansion. Another method presented in Yang et al. (2020) introduces a new hypergraph expansion called line expansion (LE) that treats vertices and hyperedges equally. The LE bijectively induces a homogeneous structure from the hypergraph by modeling vertex-hyperedge pairs. In addition, the LE and CE techniques require significant computational resources to transform the original hypergraph into a graph and perform subsequent computations, hence making the methods unpractical for large hypergraphs.

Another line of research explores hypergraph modeling involving a two-stage procedure: information is transmitted from nodes to hyperedges and then back from hyperedges to nodes (Wei et al., 2021; Yi & Park, 2020; Dong et al., 2020; Arya et al., 2020; Huang & Yang, 2021; Yadati et al., 2020). This procedure can be viewed as a two-step message passing mechanism. HyperSAGE (Arya et al., 2020) is a prominent early example of this line of research allowing transductive and inductive learning over hypergraphs. Although HyperSAGE has shown improvement in capturing information from hypergraph structures compared to spectral-based methods, it involves only one learnable linear transformation and cannot model arbitrary multiset function (Chien et al., 2022). Moreover, the algorithm utilizes nested loops resulting in inefficient computation and poor parallelism.

UniGNN (Huang & Yang, 2021) addresses some of these limitations by using a permutation-invariant function to aggregate vertex features within each hyperedge in the first stage and using learnable weights only during the second stage to update each vertex with its incident hyperedges. One of the variations of UniGNN, called UniGCNII addresses the oversmoothing problem, which is common for most of the methods described above. It accomplishes this by adapting GCNII (Chen et al., 2020) to hypergraphs. The AllSet method, proposed in Chien et al. (2022), employs a composition of two learnable multiset functions to model hypergraphs. It presents two model variations: the first one exploits Deep Set (Zaheer et al., 2017) and the second one Set Transformer (Lee et al., 2019). The AllSet method can be seen as a generalization of the most commonly used hypergraph HGNNs (Yadati et al., 2019; Feng et al., 2019; Bai et al., 2021; Dong et al., 2020; Arya et al., 2020). More implementation details and detailed drawbacks discussion can be found in Section 4.1. Although AllSet achieves state-of-the-art results, it suffers from the drawbacks of the message passing mechanism, including the local receptive field, resulting in a limited ability to model long-range interactions (Gu et al., 2020; Balcilar et al., 2021). Two additional issues are poor scalability to large hypergraph structures and oversmoothing that occurs when multiple layers are stacked.

Other lines of research target special hypergraph networks: HGTN (Li et al., 2022b) mainly focuses on heterogeneous information networks that contain different types of nodes or edges that fall out of the scope of this study. However, their method exploits the hypergraph adjacency matrix, which represents the connection relationships. MPNN-R (Yadati, 2020) extends the message passing framework to handle recursively-structured data. More recently, Wang et al. (2023) introduces ED-HNN, a novel approach for approximating continuous equivariant hypergraph diffusion operators. Its implementation is achieved through the combination of star expansions of hypergraphs with standard message passing neural networks.

## B DETAILS OF THE IMPLEMENTED METHODS

We provide a detailed overview of the models analyzed and tested in this work. In order to make their similarities and differences more evident, we express their update steps through a standard and unified notation.

**Notation** A hypergraph with  $n$  nodes and  $m$  hyperedges can be represented by an incidence matrix  $\mathbf{H} \in \mathbb{R}^{n \times m}$ . If the hyperedge  $e_j$  is incident to a node  $v_i$  (meaning  $v_i \in e_j$ ), the entry in the incidence matrix  $H_{i,j}$  is set to 1. Instead, if  $v_i \notin e_j$ , then  $H_{i,j} = 0$ .

We denote with  $\mathbf{W}$  and  $\mathbf{b}$  a learnable weight matrix and bias of a neural network, respectively. Generally,  $\mathbf{x}_v$  and  $\mathbf{z}_e$  are used to denote features for a node  $v$  and a hyperedge  $e$  respectively. Stacking all node features together we obtain the node feature matrix  $\mathbf{X}$ , while  $\mathbf{Z}$  is instead the hyperedge feature matrix.  $\sigma(\cdot)$  indicates a nonlinear activation function (such as ReLU, ELU or LeakyReLU) that depends on the model used. Finally, we use  $\parallel$  to denote concatenation.

### B.1 ALLSET-LIKE MODELS

This Section addresses the models that are covered in the AllSet unified framework introduced in 4.1, and that can potentially be expressed as particular instances of equations 4 and 6. For a detailed proof of the claim for most of the following models, refer to Theorem 3.4 in Chien et al. (2022).

#### CEGCN / CEGAT

As introduced in the previous Sections, the CE of a hypergraph  $\mathcal{G} = (\mathcal{V}, \mathcal{E})$  is a weighted graph obtained from  $\mathcal{G}$  with the same set of nodes. In terms of incidence matrix, it can be described as  $\mathbf{H}^{(CE)} = \mathbf{H}\mathbf{H}^T$  (Chien et al., 2022). A one-step update of the node feature matrix  $\mathbf{X} \in \mathbb{R}^{n \times f}$  can be expressed both in a compact way as  $\mathbf{H}^{(CE)}\mathbf{X}$  or directly as a node-level update rule, as

$$\mathbf{x}_v^{(t+1)} = \sum_{e \in \mathcal{E}_v} \sum_{u: u \in e} \mathbf{x}_u^{(t)}. \quad (13)$$

Some types of hypergraph convolutional layers in the literature adopt a CE-based propagation, for example generalizing popular graph-targeting models such as Graph Convolutional Networks (Kipf & Welling, 2017) and Graph Attention Networks (Veličković et al., 2017).

#### HGNN

Before describing how HGNN (Feng et al., 2019) works, it is necessary to define some notation. Let  $\mathbf{H}$  be the hypergraph’s incidence matrix. Suppose that each hyperedge  $e \in \mathcal{E}$  is assigned a fixed positive weight  $z_e$ , and let  $\mathbf{Z} \in \mathbb{R}^{m \times m}$  now denote the matrix stacking all these weights in the diagonal entries. Additionally, the vertex degree is defined as

$$d_v = \sum_{e \in \mathcal{E}_v} z_e \quad (14)$$

while the hyperedge degree, instead, is

$$b_e = \sum_{v: v \in e} 1. \quad (15)$$

The degree values can be used to define two diagonal matrices,  $\mathbf{D} \in \mathbb{R}^{n \times n}$  and  $\mathbf{B} \in \mathbb{R}^{m \times m}$ . The core of the hypergraph convolution introduced in Feng et al. (2019) can be expressed as

$$\mathbf{x}_v^{(t+1)} = \sigma \left( \sum_{e \in \mathcal{E}_v} \sum_{u: u \in e} z_e \mathbf{x}_u^{(t)} \mathbf{W}^{(t)} \right) \quad (16)$$

where  $\sigma$  is a non-linear activation function like LeakyReLU and ELU, and  $\mathbf{W}^{(t)} \in \mathbb{R}^{f^{(t)} \times f^{(t+1)}}$  is a weight matrix between the  $(t)$ -th and  $(t+1)$ -th layer, to be learnt during training. Note that in this case the dimensionality of the node feature vectors  $f^{(t)}$  can be layer-dependent.

The update step can be rewritten also in matrix form as

$$\mathbf{X}^{(t+1)} = \sigma(\mathbf{H} \mathbf{Z} \mathbf{H}^T \mathbf{X}^{(t)} \mathbf{W}^{(t)}), \quad (17)$$

where  $\mathbf{X}^{(t+1)} \in \mathbb{R}^{n \times f^{(t+1)}}$  and  $\mathbf{X}^{(t)} \in \mathbb{R}^{n \times f^{(t)}}$ .

In practice, a normalized version of this update procedure is proposed. The matrix-based formulation allows to clearly express the symmetric normalization that is actually put in place through the vertex and hyperedge degree matrices  $\mathbf{D}$  and  $\mathbf{B}$  defined above:

$$\mathbf{X}^{(t+1)} = \sigma(\mathbf{D}^{-1/2} \mathbf{H} \mathbf{Z} \mathbf{B}^{-1} \mathbf{H}^T \mathbf{D}^{-1/2} \mathbf{X}^{(t)} \mathbf{W}^{(t)}). \quad (18)$$

## HCHA

With respect to the previously described models, HCHA (Bai et al., 2021) uses a different kind of weights that depend on the node and hyperedge features. Specifically, starting from the same convolutional model proposed by Feng et al. (2019) and described in Equation 18, they explore the idea of introducing an attention learning model on  $\mathbf{H}$ .

Their starting point is the intuition that hypergraph convolution as implemented in Equation 18 implicitly puts in place some attentional mechanism, which derives from the fact that the afferent and efferent information flow to vertices may be assigned different importance levels, which are statically encoded in the incidence matrix  $\mathbf{H}$ , hence depend only on the graph structure. In order to allow for such information on magnitude of importance to be determined dynamically and possibly vary from layer to layer, they introduce an attention learning module on the incidence matrix  $\mathbf{H}$ : instead of maintaining  $\mathbf{H}$  as a binary matrix with predefined and fixed entries depending on the hypergraph connectivity, they suggest that its entries could be learnt during the training process. The entries of the matrix should express a probability distribution describing the degree of node-hyperedge connectivity, through non-binary and real values.

Nevertheless, the proposed hypergraph attention is only feasible when the hyperedge and vertex sets share the same homogeneous domain, otherwise, their similarities would not be compatible. In case the comparison is feasible, the computation of attentional scores is inspired by (Veličković et al., 2017): for a given vertex  $v$  and a hyperedge  $e$ , the score is computed as

$$H_{v,e} = \frac{\exp(\sigma(\text{sim}(\mathbf{x}_v \mathbf{W}, \mathbf{z}_e \mathbf{W})))}{\sum_{g \in \mathcal{E}_v} \exp(\sigma(\text{sim}(\mathbf{x}_v \mathbf{W}, \mathbf{z}_g \mathbf{W})))}, \quad (19)$$

where  $\sigma$  is a non-linear activation function, and  $\text{sim}$  is a similarity function defined as

$$\text{sim}(\mathbf{x}_v, \mathbf{z}_e) = \mathbf{a}^T [\mathbf{x}_v \parallel \mathbf{z}_e] \quad (20)$$

in which  $\mathbf{a}$  is a weight vector, and the resulting similarity value is a scalar.

## HyperGCN

The method proposed by Yadati et al. (2019) can be described as performing two steps sequentially: first, a graph structure is defined starting from the input hypergraph, through a particular procedure,

and then the well known CGN model (Kipf & Welling, 2017) for standard graph structures is executed on it. Depending on the approach followed in the first step, three slight variations of the same model can be identified: 1-HyperGCN, HyperGCN (enhancing 1-HyperGCN with so-called *mediators*) and FastHyperGCN.

Before analyzing the differences among the three techniques, we introduce some notation and express how the GCN-update step is performed. Suppose that the input hypergraph  $\mathcal{G} = (\mathcal{V}, \mathcal{E})$  is equipped with initial edge weights  $\{z_e\}_{e \in \mathcal{E}}$  and node features  $\{\mathbf{x}_v\}_{v \in \mathcal{V}}$  (if missing, suppose to initialize them randomly or with constant values). Let  $\bar{\mathbf{A}}^{(t)}$  denote the normalized adjacency matrix associated to the graph structure at time-step  $(t)$ . The node-level one-step update for a specific node  $v$  can be formalized as:

$$\mathbf{x}_v^{(t+1)} = \sigma \left( \left( \mathbf{W}^{(t)} \right)^T \sum_{u \in \mathcal{N}_v} \bar{\mathbf{A}}_{u,v}^{(t)} \cdot \mathbf{x}_u^{(t)} \right) \quad (21)$$

in which  $\mathbf{x}_v^{(t+1)}$  is the  $(t+1)$ -th step hidden representation of node  $v$  and  $\mathcal{N}_v$  is the set of neighbors of  $v$ . For what concerns  $\bar{\mathbf{A}}_{u,v}^{(t)}$ , it refers to the element at index  $u, v$  of  $\bar{\mathbf{A}}^{(t)}$ , which can be defined in the following ways according to the method:

1. 1-HyperGCN: starting from the hypergraph  $\mathcal{G} = (\mathcal{V}, \mathcal{E})$ , a simple graph is defined by considering exactly one representative simple edge for each hyperedge  $e \in \mathcal{E}$ , and it is defined as  $(v_e, u_e)$  such that  $(v_e, u_e) = \operatorname{argmax}_{v, u \in e} \|(\mathbf{W}^{(t)})^T (\mathbf{x}_v^{(t)} - \mathbf{x}_u^{(t)})\|_2$ . This implies that each hyperedge  $e$  is represented by just one pairwise edge  $(v_e, u_e)$ , and this may also change from one step to the other, which leads to the graph adjacency matrix  $\bar{\mathbf{A}}^{(t)}$  being layer-dependent, too.
2. HyperGCN: the model extends the graph construction procedure of 1-HyperGCN by also considering *mediator* nodes, that for each hyperedge  $e$  consist in  $K_e := \{k \in e : k \neq v_e, k \neq u_e\}$ . Once the representative edge  $(v_e, u_e)$  is determined and added to the newly defined graph, two edges for each mediator are also introduced, connecting the mediator to both  $v_e$  and  $u_e$ . Because there are  $2|e| - 3$  edges for each hyperedge  $e$ , each weight is chosen to be  $\frac{1}{2|e|-3}$  in order for the weights in each hyperedge to sum to 1. The generalized Laplacian obtained this way satisfies all the properties of the HyperGCN’s Laplacian (Yadati et al., 2019).
3. FastHyperGCN: in order to save training time, in this case the adjacency matrix  $\bar{\mathbf{A}}^{(t)}$  is computed only once before training, by using only the initial node features of the input hypergraph.

## UniGCNII

This model aims to extend to hypergraph structures the GCNII model proposed by Chen et al. (2020) for simple graph structures, that is a deep graph convolutional network that puts in place an initial residual connection and identity mapping as a way to reduce the oversmoothing problem (Huang & Yang, 2021).

Let  $d_v$  denote the degree of vertex  $v$ , while  $d_e = \frac{1}{|e|} \sum_{i \in e} d_i$  for each hyperedge  $e \in \mathcal{E}$ . A single node-level update step performed by UniGCNII can be expressed as:

$$\hat{\mathbf{x}}_v^{(t)} = \frac{1}{\sqrt{d_v}} \sum_{e \in \mathcal{E}_v} \frac{z_e^{(t)}}{\sqrt{d_e}}, \quad (22)$$

$$\mathbf{x}_v^{(t+1)} = ((1 - \beta)\mathbf{I} + \beta\mathbf{W}^{(t)})((1 - \alpha)\hat{\mathbf{x}}_v^{(t)} + \alpha\mathbf{x}_v^{(0)}) \quad (23)$$

in which  $\alpha$  and  $\beta$  are hyperparameters,  $\mathbf{I}$  is identity matrix and  $\mathbf{x}_v^{(0)}$  is the initial feature of vertex  $i$ .

## HNHN

For the HNHN model by Dong et al. (2020), hypernode and hyperedge features are supposed to share the same dimensionality  $d$ , hence in this case  $\mathbf{X} \in \mathbb{R}^{n \times d}$  and  $\mathbf{Z} \in \mathbb{R}^{m \times d}$ . The update rule in this case can be easily expressed using the incidence matrix as

$$\mathbf{Z}^{(t+1)} = \sigma(\mathbf{H}^T \mathbf{X}^{(t)} \mathbf{W}_Z + \mathbf{b}_Z) \quad (24)$$

$$\mathbf{X}^{(t+1)} = \sigma(\mathbf{H} \mathbf{Z}^{(t+1)} \mathbf{W}_X + \mathbf{b}_X) \quad (25)$$

in which  $\sigma$  is a nonlinear activation function,  $\mathbf{W}_X, \mathbf{W}_Z \in \mathbb{R}^{d \times d}$  are weight matrices, and  $\mathbf{b}_X, \mathbf{b}_Z \in \mathbb{R}^d$  are bias terms.

### AllSet

The general formulation for the propagation setting of AllSet (Chien et al., 2022) is introduced in Subsection 4.1 and, starting from that, we now analyze the different instances of the model obtained by imposing specific design choices in the general framework.

In the practical implementation of the model, the update functions  $f_{\mathcal{V} \rightarrow \mathcal{E}}$  and  $f_{\mathcal{E} \rightarrow \mathcal{V}}$ , that are required to be permutation invariant with respect to their first input, are parametrized and *learned* for each dataset and task. Furthermore, the information of their second argument is not utilized in practice, hence their input can be more generally denoted as a set  $\mathbb{S}$ .

The two architectures AllDeepSets and AllSetTransformer are obtained in the following way, depending on whether the update functions are defined either as MLPs or Transformers:

1. AllDeepSets (Chien et al., 2022):  $f_{\mathcal{V} \rightarrow \mathcal{E}}(\mathbb{S}) = f_{\mathcal{E} \rightarrow \mathcal{V}}(\mathbb{S}) = \text{MLP}(\sum_{s \in \mathbb{S}} \text{MLP}(s))$ ;
2. AllSetTransformer (Chien et al., 2022), in which the update functions are defined iteratively through multiple steps as they were first designed by Vaswani et al. (2017).

The first set of operations corresponds to the self-attention module. Suppose that  $h$  attention heads are considered: first of all,  $h$  pairs of matrices  $\mathbf{K}_i$  (keys) and  $\mathbf{V}_i$  (values) with  $i \in \{1, \dots, h\}$  are computed from the input set through different MLPs. Additionally,  $h$  weights  $\theta_i, i \in \{1, \dots, h\}$  are also learned and together with the keys and values they allow for the computation of each head-specific attention value  $\mathbf{O}_i$  using an activation function  $\omega$  (Vaswani et al., 2017). The  $h$  attention heads are processed in parallel and they are then concatenated, leading to a unique vector being the result of the multi-head attention module  $\text{MH}_{h,\omega}$ . After that, a sum operation and a Layer Normalization (LN) (Ba et al., 2016) are applied:

$$\mathbf{K}_i = \text{MLP}_i^K(\mathbb{S}), \mathbf{V}_i = \text{MLP}_i^V(\mathbb{S}), \quad \text{where } i \in \{1, \dots, h\}, \quad (26)$$

$$\theta \triangleq \parallel_{i=1}^h \theta_i, \quad (27)$$

$$\mathbf{O}_i = \omega(\theta_i (\mathbf{K}_i)^T) \mathbf{V}_i, \quad \text{where } i \in \{1, \dots, h\}, \quad (28)$$

$$\text{MH}_{h,\omega}(\theta, \mathbb{S}, \mathbb{S}) = \parallel_{i=1}^h \mathbf{O}^{(i)}, \quad (29)$$

$$\mathbf{Y} = \text{LN}(\theta + \text{MH}_{h,\omega}(\theta, \mathbb{S}, \mathbb{S})) \quad (30)$$

A feed-forward module follows the self-attention computations, in which a MLP is applied to the feature matrix and then sum and LN are performed again, corresponding to the last operations to be performed:

$$f_{\mathcal{V} \rightarrow \mathcal{E}}(\mathbb{S}) = f_{\mathcal{E} \rightarrow \mathcal{V}}(\mathbb{S}) = \text{LN}(\mathbf{Y} + \text{MLP}(\mathbf{Y})) \quad (31)$$

## B.2 OTHER MODELS

This Section describes the models that are considered for the experiments but that don't fall directly under the AllSet unified framework defined in Section 4.1.

### HAN

The Heterogeneous Graph Attention Network model (Wang et al., 2019) is specifically designed for processing and performing inference on heterogeneous graphs. Heterogeneous graphs have various

types of nodes and/or edges, and standard GNN models that treat all of them equally are not able to properly handle such complex information.

In order to apply this model on hypergraphs, (Chien et al., 2022) define a preprocessing step to derive a heterogeneous graph from a hypergraph. Specifically, a bipartite graph is defined such that there is a bijection between its nodes and the set of nodes and hyperedges in the original hypergraph. The nodes obtained in this way belong to one of two distinct types, that are the sets  $\mathbb{V}$  and  $\mathbb{E}$  (if they correspond to either a node or a hyperedge in the original hypergraph, respectively). Edges only connect nodes of two different types, and one edge exists between a node  $u_v \in \mathbb{V}$  and a node  $u_e \in \mathbb{E}$  if and only if  $v \in e$  in the input hypergraph. We consider two types of so-called meta-paths (in this case, paths of length 2) in the heterogeneous graph, that are  $\mathbb{V} \rightarrow \mathbb{E} \rightarrow \mathbb{V}$  and  $\mathbb{E} \rightarrow \mathbb{V} \rightarrow \mathbb{E}$ . We denote the sets of such meta-paths as  $\Phi_{\mathbb{V}}$  and  $\Phi_{\mathbb{E}}$  respectively. Furthermore, let  $\mathcal{N}_{u_v}^{\Phi_{\mathbb{V}}}$  denote the neighbors of node  $u_v \in \mathbb{V}$  through paths  $\gamma_v \in \Phi_{\mathbb{V}}$ , and viceversa let  $\mathcal{N}_{u_e}^{\Phi_{\mathbb{E}}}$  denote the neighbors of node  $u_e \in \mathbb{E}$  through paths  $\gamma_e \in \Phi_{\mathbb{V}}$ .

At each step, the model updates separately and sequentially the node features of nodes in  $\mathbb{V}$  and  $\mathbb{E}$ . Consider for example the case of nodes in  $\mathbb{V}$  (for nodes in  $\mathbb{E}$  the process is the same, except that  $\Phi_{\mathbb{E}}$  is considered instead of  $\Phi_{\mathbb{V}}$ ). The node-level update is performed as follows, for a certain  $u \in \mathbb{V}$ :

$$\hat{\mathbf{x}}_u^{(t)} = \mathbf{W}_{\Phi_{\mathbb{V}}}^{(t)} \mathbf{x}_u^{(t)}, \quad (32)$$

$$\mathbf{x}_u^{(t+1)} = \sigma \left( \sum_{w \in \mathcal{N}_u^{\Phi_{\mathbb{V}}}} \alpha_{u,w}^{\Phi_{\mathbb{V}}} \hat{\mathbf{x}}_w^{(t)} \right) \quad (33)$$

In the equations above,  $\mathbf{W}_{\Phi_{\mathbb{V}}}^{(t)}$  is a meta-path dependent weight matrix while  $\alpha_{u,w}^{\Phi_{\mathbb{V}}}$  is an attentional score computed between neighboring nodes in the same way as proposed in Veličković et al. (2017), through similar equations as 19 and 20. More generally,  $h$  attention heads may be considered, that give rise to different attentional scores for each head and consequently multiple results for the node feature update, that are then concatenated to obtain a unique feature vector  $\mathbf{x}_u^{(t+1)}$ .

### MLP

We also add the MLP model as a baseline; this model doesn't use connectivity at all and only relies on the initial node features to predict their class. The node feature matrix  $\mathbf{X}$  is obtained as

$$\mathbf{X}^{(t)} = \text{MLP}(\mathbf{X}^{(t-1)}) \quad (34)$$

### MMLP CB

MMLP stands for Multiple-Multilayer-Perceptrons, and it is an additional baseline model we implemented in order to test whether improving the results is achievable by deploying different tailored MLPs for different connectivity values.

In particular, 4 different MLPs are learned: 3 of them target the overall top-3 connectivity levels, while the 4th one deals with all other connectivity values.

### MLP CB

This model, in contrast to its counterparts, employs a sampling procedure as outlined in Section 4.2. In this procedure, we straightforwardly apply a Multilayer Perceptron to the initial features of nodes. During the training phase, we incorporate dropout by applying an MLP with distinct weights dropped out for each hyperedge, resulting in slightly different representations for nodes for each hyperedge they belong to. Furthermore, we execute the mini-batching procedure in accordance with the guidelines presented in Section 4.2. It is important to note that these two choices affect the training approach significantly so that the results of this model are very different from MLP's performances: see, for example, Table 1.

During the validation phase, dropout is not utilized, ensuring that the representations used for each hyperedge remain exactly the same. Consequently, there is no need for the readout operation in this context. Let  $d_v$  denote the degree of vertex  $v$ ; the node-level update is then described by:

$$\mathbf{x}_{v,e}^{(t+1)} = \mathbf{x}_{v,e}^{(t)} + \text{MLP}(\text{LN}(\mathbf{x}_{v,e}^{(t)})) \quad (35)$$

$$\mathbf{x}_v^{(T)} = \frac{1}{d_v} \sum_{e \in \mathcal{E}_v} \mathbf{x}_{v,e}^{(T)} \quad (36)$$

## Transformer

Along with MLP, we consider another simple baseline that is the basic Transformer model (Vaswani et al., 2017).

Also in this case, let  $\mathbb{S}$  denote the set of input vectors, and define as  $\mathbf{S} = \text{MLP}(\mathbb{S})$  the matrix of input embeddings, obtained from the input set through a MLP. The operations performed on  $\mathbf{S}$  generalize the ones described for the Transformer module adopted in AllSetTransformer, and they can be split in two main modules, that are the self-attention module and the feed-forward module:

1. Suppose that  $h$  attention heads are considered in the self attention module. First of all,  $h$  triples of matrices  $\mathbf{K}_i$  (keys),  $\mathbf{V}_i$  (values) and  $\mathbf{Q}_i$  (queries) with  $i \in \{1, \dots, h\}$  are obtained from  $\mathbf{S}$  through linear matrix multiplications with weight matrices  $\mathbf{W}_i^K$ ,  $\mathbf{W}_i^V$  and  $\mathbf{W}_i^Q$  that are learned during training. The result for each attention module is computed through the key, query and key matrices using an activation function  $\omega$  (Vaswani et al., 2017) and a normalization factor  $d_k$ , that corresponds to the dimension of the key and query vectors associated to each input element. The  $h$  outputs of the different attention heads are then concatenated, leading to a unique result matrix. After that, a sum operation and a Layer Normalization (LN) (Ba et al., 2016) are applied:

$$\mathbf{K}_i = \mathbf{S}\mathbf{W}_i^K, \mathbf{V}_i = \mathbf{S}\mathbf{W}_i^V, \mathbf{Q}_i = \mathbf{S}\mathbf{W}_i^Q, \quad \text{where } i \in \{1, \dots, h\}, \quad (37)$$

$$\mathbf{O}_i = \omega \left( \frac{\mathbf{Q}_i(\mathbf{K}_i)^T}{\sqrt{d_k}} \right) \mathbf{V}_i, \quad \text{where } i \in \{1, \dots, h\}, \quad (38)$$

$$\text{MH}_{h,\omega}(\mathbf{S}, \mathbf{S}) = \|\|_{i=1}^h \mathbf{O}^{(i)}, \quad (39)$$

$$\mathbf{Y} = \text{LN}(\mathbf{S} + \text{MH}_{h,\omega}(\mathbf{S}, \mathbf{S})) \quad (40)$$

2. As described for AllSetTransformer (Chien et al., 2022), in the feed-forward module a MLP is applied to the feature matrix, followed by a sum operation and Layer Normalization. After that, the output of the overall Transformer architecture is obtained:

$$\mathbf{Y}_{out} = \text{LN}(\mathbf{Y} + \text{MLP}(\mathbf{Y})). \quad (41)$$

## C PROOF OF PROPOSITION 1

UniGCNII inherits the same hyperedge update rule of other hypergraph models (e.g. HGNN (Feng et al., 2019), HyperGCN (Yadati et al., 2019)), so it directly follows from Theorem 3.4 of (Chien et al., 2022) that it can be expressed through 4. By looking at the definition of the node update rule of UniGCNII (Eq. 22 and 23), we can re-express it as

$$\mathbf{x}_v^{(t+1)} = ((1-\beta)\mathbf{I} + \beta\mathbf{W}^{(t)}) \left( (1-\alpha) \frac{1}{\sqrt{d_v}} \sum_{e \in \mathcal{E}_v} \frac{\mathbf{z}_e^{(t+1)}}{\sqrt{d_e}} + \alpha \mathbf{x}_v^{(0)} \right) = f_{\mathcal{E} \rightarrow \mathcal{V}}(\{\mathbf{z}_e^{(t+1)}\}_{e \in \mathcal{E}_v}; \mathbf{x}_v^{(0)}). \quad (42)$$

Note that this is a particular instance of the extended AllSet node update rule 6 where only a residual connection to the initial node features is considered. Lastly, it is straightforward to see that  $f_{\mathcal{E} \rightarrow \mathcal{V}}$  is permutation invariant w.r.t the set  $\{\mathbf{z}_e^{(t+1)}\}_{e \in \mathcal{E}_v}$ , as it processes the set through a weighted mean.  $\square$

---

## D PROOF OF PROPOSITION 2

We prove this proposition by showing that we can obtain AllSet update rules 4-5 and 6 from our proposed MultiSet framework 7-8-9. This can easily follow by not distinguishing node representations among hyperedges, so  $\mathbb{X}_v^{(t)} = \{\mathbf{x}_{v,e}^{(t)}\}_{e \in \mathcal{E}_v} = x_v^{(t)}$ . With this particular choice, we directly get 4 from 7, and 6 can be obtained from 8 by further disregarding the hyperedge subscript –as there is only a single node representation to update. Analogously, we can get 5 from 8 if we additionally do not consider node residual connections, so  $\{\mathbb{X}_v^{(k)}\}_{k=0}^t$  simply becomes  $x_v^{(t)}$ . Finally, the readout 9 can be defined as the identity function applied to the node representations at the last message passing step  $T$ .  $\square$

## E PROOF OF PROPOSITION 3

It is straightforward that functions  $f_{\mathcal{V} \rightarrow \mathcal{E}}$ ,  $f_{\mathcal{E} \rightarrow \mathcal{V}}$  and  $f_{\mathcal{V} \rightarrow \mathcal{V}}$  defined in MultiSetMixer (Equations 10-12) are permutation invariant w.r.t their first argument: hyperedge update rule 10 and readout 12 process it through a mean operation, whereas the node update rule only receives a single-element set. The rest of the proof follows from the proof of Proposition 4.1 of Chien et al. (2022).  $\square$

## F EXPERIMENTS

### F.1 HYPERPARAMETERS OPTIMIZATION

In order to implement the benchmark models, we followed the procedure described in Chien et al. (2022); in particular, the maximum epochs were set to 200 for all the models. The models were trained with categorical cross-entropy loss, and the best architecture was selected at the end of training depending on validation accuracy. For the AllDeepSets (Chien et al., 2022), AllSetTransformer (Chien et al., 2022), UniGCNII (Huang & Yang, 2021), CEGAT, CEGCN, HCHA (Bai et al., 2021), HGNN (Feng et al., 2019), HNHN (Dong et al., 2020), HyperGCN (Yadati et al., 2019), HAN(Wang et al., 2019), and HAN (mini-batching) (Wang et al., 2019) and MLP, we performed the same hyperparameter optimization proposed in Chien et al. (2022). For both the proposed model and the introduced baseline, we conducted a thorough hyperparameter search across the following possibilities:

- Learning rate within the range of 0.001, 0.01
- Weight decay values from the set 0.0,  $1e - 5$ , 1
- MLP hidden layer sizes of 64, 128, 256, 512
- Mini-batch sizes set to 256, 512, with full-batch utilization when memory resources allow
- The number of sampled neighbors per hyperedge ranged from 2, 3, 5, 10.

It’s important to note that the limitation of the number of sampled neighbors per hyperedge to this small range was intentional. This limitation showcases that even for datasets with large hyperedges, effective processing can be achieved by considering only a subset of neighbors.

The models’ hyperparameters were optimized for a 50% split and subsequently applied to all the other splits.

### F.2 FURTHER INFORMATION ABOUT THE DATASETS

For our experiments we utilized various benchmark datasets from existing literature on hypergraph neural networks. For what concerns co-authorship networks (Cora-CA and DPBL-CA) and co-citation networks (Cora, Citeseer, and Pubmed), we relied on the datasets provided in (Yadati et al., 2019). Additionally, we employed the Princeton ModelNet40 (Wu et al., 2015) and the National Taiwan University (Chen et al., 2003) dataset introduced for 3D object classification. For these two datasets, we complied with what (Feng et al., 2019) and (Yang et al., 2020) proposed for the construction of the hypergraphs, using both MVCNN (Su et al., 2015) and GVCNN (Feng et al., 2019) features. Additionally, we tested our model on three datasets with categorical attributes, namely 20Newsgroups,

Mushroom, and ZOO, obtained from the UCI Categorical Machine Learning Repository (Dua et al., 2017). In order to construct hypergraphs for these datasets, we followed the approach described in (Yadati et al., 2019), where a hyperedge is defined for all data points sharing the same categorical feature value.

Table 5: Statistics of hypergraph datasets:  $|e|$  denotes the size of hyperedges while  $d_v$  denotes the node degree

	Cora	Citeseer	Pubmed	CORACA	DBLP-CA	ZOO	20Newsgroups	Mushroom	NTU2012	ModelNet40
# classes	7	6	3	7	6	7	4	2	67	40
min $ e $	2	2	2	2	2	1	29	1	5	5
med $ e $	3	2	3	3	3	40	537	72	5	5
max $d_v$	145	88	99	23	18	17	44	5	19	30
min $d_v$	0	0	0	0	1	17	1	5	1	1
avg $d_v$	1.77	1.04	1.76	1.69	2.41	17	4.03	5	5	5
med $d_v$	1	0	0	2	2	17	3	5	5	4

We downloaded co-citation and co-authoring networks from (Yadati et al., 2019). Below are the details on how the hypergraph was constructed. **Cora-CA, DBLP**: all documents co-authored by an author are in one hyperedge, following what was done in (Yadati et al., 2019). Co-citation data **Citeseer, Pubmed, Cora**: all documents cited by a document are connected by a hyperedge. Each hypernode (document abstract) is represented by bag-of-words features (feature matrix  $X$ ).

**Citation and co-authorship datasets** In the co-citation and co-authorship networks datasets, the node features are the bag-of-words representations of the corresponding documents. In co-citation datasets (Cora, Citeseer, PubMed) all documents cited by a document are connected by a hyperedge. In co-authored datasets (CORA-CA, DBLP-CA), all documents co-authored by an author belong to the same hyperedge.

**Computer vision/graphics** The hyperedges are constructed using the  $k$ -nearest neighbor algorithm in which  $k = 5$ .

**Categorical datasets** There are instances with categorical attributes within the datasets. To construct the hypergraph, each attribute value is treated as a hyperedge, meaning that all instances (hypernodes) with the same attribute value are contained in a hyperedge. The node features of 20Newsgroups are the TF-IDF representations of news messages. The node features of mushrooms (in Mushroom dataset) represent categorical descriptions of 23 species. The node features of a zoo (in ZOO dataset) are a combination of categorical and numeric measurements describing various animals.

Table 6: Node Connectivity Statistics. For brevity we use the following notation in this table: under the columns labeled  $|\mathcal{E}_v| = k$ , we report the amount of nodes that belong to  $k$  hyperedges. This value can be expressed in a more formal way as  $|v \in \mathcal{V} : |\mathcal{E}_v| = k|$ . Moreover,  $|\mathcal{E}_v| = 0$ , denotes the number of isolated nodes. In addition, the columns labeled “%  $|\mathcal{E}_v| = k$ ” indicate the percentage of nodes belonging to  $k$  hyperedges relatively to the total number of nodes.

	$ \mathcal{V} $	$ \mathcal{E}_v  = 0$	$ \mathcal{E}_v  = 1$	$ \{v :  \mathcal{E}_v  = 2\} $	$ \mathcal{E}_v  = 3$	$ \mathcal{E}_v  > 3$	% $ \mathcal{E}_v  = 0$	% $ \mathcal{E}_v  = 1$	% $ \mathcal{E}_v  = 2$	% $ \mathcal{E}_v  = 3$	% $ \mathcal{E}_v  > 3$
Cora	2708	1274	575	327	156	376	47.05	21.23	12.08	5.76	13.88
Citeseer	3312	1854	798	307	144	209	55.98	24.09	9.27	4.35	6.31
Pubmed	19717	15877	339	313	292	2896	80.52	1.72	1.59	1.48	14.69
CORA-CA	2708	320	995	951	287	155	11.82	36.74	35.12	10.60	5.72
DBLP-CA	41302	0	8998	16724	9249	6331	0.00	21.79	40.49	22.39	15.33
Mushroom	8124	0	0	0	0	8124	0.00	0.00	0.00	0.00	100.00
NTU2012	2012	0	173	256	296	1287	0.00	8.60	12.72	14.71	63.97
ModelNet40	12311	0	1491	1755	1594	7471	0.00	12.11	14.26	12.95	60.69
20newsW100	16242	0	3053	3149	2720	7320	0.00	18.80	19.39	16.75	45.07
ZOO	101	0	0	0	0	101	0.00	0.00	0.00	0.00	100.00

Table 7: Hypergraph model performance benchmarks. Test accuracy in % averaged over 15 splits. Training split: 50%.

Model	Cora	Citeseer	Pubmed	CORA-CA	DBLP-CA	Mushroom	NTU2012	ModelNet40	20Newsgroups	ZOO	avg. ranking
AllDeepSets	77.11 ± 1.00	70.67 ± 1.42	<b>89.04 ± 0.45</b>	82.23 ± 1.46	91.34 ± 0.27	99.96 ± 0.05	86.49 ± 1.86	96.70 ± 0.25	81.19 ± 0.49	89.10 ± 7.00	6.00
AllSetTransformer	<b>79.54 ± 1.02</b>	72.52 ± 0.88	88.74 ± 0.51	<b>84.43 ± 1.14</b>	<b>91.61 ± 0.19</b>	99.95 ± 0.05	88.22 ± 1.42	<b>98.00 ± 0.12</b>	81.59 ± 0.59	<b>91.03 ± 7.31</b>	<b>2.85</b>
UniGCNII	78.46 ± 1.14	<b>73.05 ± 1.48</b>	88.07 ± 0.47	<b>83.92 ± 1.02</b>	<b>91.56 ± 0.18</b>	99.89 ± 0.07	88.24 ± 1.56	97.84 ± 0.16	81.16 ± 0.49	<b>89.61 ± 8.09</b>	4.15
CEGAT	76.53 ± 1.58	75.58 ± 1.11	87.11 ± 0.49	75.50 ± 1.51	88.74 ± 0.31	96.81 ± 0.44	82.27 ± 1.60	92.79 ± 0.44	nan	44.62 ± 1.18	11.00
CEGCN	77.03 ± 1.31	70.87 ± 1.19	87.01 ± 0.62	77.55 ± 1.65	88.12 ± 0.25	94.91 ± 0.44	80.90 ± 1.74	90.04 ± 0.47	nan	49.23 ± 6.81	11.67
HCHA	<b>79.53 ± 1.33</b>	72.57 ± 1.06	86.97 ± 0.55	<b>83.53 ± 1.12</b>	91.21 ± 0.28	98.94 ± 0.54	86.60 ± 1.96	94.50 ± 0.33	80.75 ± 0.53	<b>89.23 ± 6.81</b>	6.75
HGNN	<b>79.53 ± 1.33</b>	72.24 ± 1.08	86.97 ± 0.55	<b>83.45 ± 1.22</b>	91.26 ± 0.26	98.94 ± 0.54	86.71 ± 1.48	94.50 ± 0.33	80.75 ± 0.52	<b>89.23 ± 6.81</b>	6.85
HNHN	77.68 ± 1.08	73.47 ± 1.36	87.88 ± 0.47	78.53 ± 1.15	86.73 ± 0.40	<b>99.97 ± 0.04</b>	<b>88.28 ± 1.50</b>	97.84 ± 0.15	81.53 ± 0.55	<b>89.23 ± 7.85</b>	5.05
HyperGCN	74.78 ± 1.11	66.06 ± 1.58	82.32 ± 0.62	77.48 ± 1.14	86.07 ± 3.32	69.51 ± 4.98	47.65 ± 5.01	46.10 ± 7.95	80.84 ± 0.49	51.54 ± 9.88	13.80
HAN	<b>80.73 ± 1.37</b>	<b>73.69 ± 0.95</b>	86.34 ± 0.61	<b>84.19 ± 0.81</b>	91.10 ± 0.20	91.33 ± 0.91	83.78 ± 1.75	93.85 ± 0.33	79.67 ± 0.55	80.26 ± 6.42	8.10
HAN minibatch	<b>80.24 ± 2.17</b>	<b>73.55 ± 1.13</b>	85.41 ± 2.32	82.04 ± 2.56	90.52 ± 0.50	93.87 ± 1.04	80.62 ± 2.00	92.06 ± 0.63	79.76 ± 0.56	70.39 ± 11.29	9.90
MultiRepMixer	79.38 ± 1.08	72.79 ± 1.12	85.71 ± 0.49	82.62 ± 1.20	89.87 ± 0.29	95.85 ± 3.21	<b>88.73 ± 1.29</b>	<b>98.15 ± 0.19</b>	<b>87.83 ± 2.68</b>	78.67 ± 9.08	6.40
MMLP CB	74.06 ± 1.26	71.93 ± 1.53	85.83 ± 0.51	74.39 ± 1.40	84.91 ± 0.44	96.83 ± 2.18	85.43 ± 1.51	96.41 ± 0.32	<b>86.13 ± 2.82</b>	81.61 ± 10.98	9.80
MMLP CB	71.05 ± 2.03	69.26 ± 1.91	85.20 ± 0.54	71.16 ± 2.17	84.08 ± 0.42	95.71 ± 2.42	nan	nan	85.04 ± 4.04	<b>83.89 ± 9.52</b>	12.75
MMLP Classic	73.27 ± 1.09	72.07 ± 1.65	87.13 ± 0.49	73.27 ± 1.09	84.77 ± 0.41	99.91 ± 0.08	79.70 ± 1.56	95.31 ± 0.28	80.93 ± 0.59	<b>85.13 ± 6.90</b>	10.40
Transformer Classic	74.15 ± 1.17	71.82 ± 1.51	87.37 ± 0.49	73.61 ± 1.55	85.26 ± 0.38	<b>99.95 ± 0.08</b>	82.88 ± 1.93	96.29 ± 0.29	81.17 ± 0.54	<b>88.72 ± 10.25</b>	9.05

Table 8: Hypergraph model performance benchmarks. Test accuracy in % averaged over 15 splits. Training split: 40%.

Model	Cora	Citeseer	Pubmed	CORA-CA	DBLP-CA	Mushroom	NTU2012	ModelNet40	20Newsgroups	ZOO	avg. ranking
AllDeepSets	76.09 ± 1.22	70.32 ± 1.39	<b>88.58 ± 0.46</b>	81.32 ± 1.27	90.96 ± 0.24	99.94 ± 0.08	85.60 ± 1.46	96.71 ± 0.21	81.11 ± 0.43	<b>89.57 ± 5.91</b>	6.30
AllSetTransformer	<b>78.81 ± 0.99</b>	71.65 ± 1.05	<b>88.17 ± 0.45</b>	<b>83.26 ± 1.12</b>	<b>91.26 ± 0.24</b>	99.94 ± 0.09	<b>87.04 ± 1.07</b>	97.92 ± 0.14	81.30 ± 0.41	<b>91.72 ± 6.38</b>	<b>3.15</b>
UniGCNII	77.78 ± 1.15	<b>72.30 ± 1.45</b>	87.86 ± 0.37	<b>83.39 ± 0.95</b>	<b>91.32 ± 0.19</b>	99.88 ± 0.09	<b>87.30 ± 1.34</b>	97.86 ± 0.16	81.14 ± 0.45	<b>89.68 ± 6.42</b>	3.55
CEGAT	75.68 ± 1.09	70.59 ± 0.89	86.39 ± 0.47	76.91 ± 1.22	88.18 ± 0.31	96.72 ± 1.50	80.97 ± 1.30	92.46 ± 0.29	nan	45.27 ± 9.41	10.67
CEGCN	76.19 ± 1.06	70.08 ± 1.26	86.22 ± 0.50	76.17 ± 1.44	87.61 ± 0.26	95.00 ± 0.38	79.41 ± 1.26	89.79 ± 0.39	nan	51.40 ± 7.24	11.83
HCHA	<b>78.87 ± 1.04</b>	71.73 ± 0.91	86.28 ± 0.43	<b>83.05 ± 0.99</b>	91.04 ± 0.23	99.00 ± 0.48	85.53 ± 1.43	94.53 ± 0.28	80.77 ± 0.31	90.54 ± 5.29	6.30
HGNN	<b>78.87 ± 1.04</b>	71.44 ± 1.00	86.28 ± 0.43	<b>82.95 ± 1.06</b>	91.06 ± 0.24	99.00 ± 0.48	85.71 ± 1.37	94.53 ± 0.28	80.77 ± 0.31	90.54 ± 5.29	6.30
HNHN	76.47 ± 0.90	<b>72.25 ± 1.10</b>	87.17 ± 0.45	77.27 ± 1.11	86.61 ± 0.31	<b>99.96 ± 0.08</b>	<b>87.14 ± 1.23</b>	97.82 ± 0.17	81.28 ± 0.49	<b>89.46 ± 6.50</b>	5.30
HyperGCN	73.56 ± 0.91	64.65 ± 1.28	82.09 ± 0.67	76.44 ± 1.06	86.22 ± 2.93	69.49 ± 5.02	46.78 ± 4.61	45.34 ± 7.34	80.82 ± 0.59	52.80 ± 9.90	13.50
HAN	<b>79.89 ± 0.78</b>	<b>73.16 ± 1.04</b>	86.11 ± 0.56	<b>83.84 ± 0.91</b>	90.96 ± 0.19	91.39 ± 0.93	82.79 ± 1.16	93.83 ± 0.27	79.52 ± 0.47	80.11 ± 6.46	7.95
HAN minibatch	<b>80.07 ± 1.68</b>	69.44 ± 6.58	86.08 ± 0.84	82.33 ± 1.91	nan	93.60 ± 0.91	79.41 ± 1.62	nan	79.43 ± 0.91	64.84 ± 12.59	10.81
MultiRepMixer	<b>78.60 ± 0.89</b>	71.75 ± 1.20	85.00 ± 0.54	81.67 ± 0.84	89.74 ± 0.27	97.76 ± 1.70	<b>87.07 ± 1.06</b>	<b>98.17 ± 0.14</b>	<b>86.85 ± 3.30</b>	79.01 ± 8.08	6.60
MMLP CB	72.60 ± 1.44	71.08 ± 1.68	85.14 ± 0.47	72.63 ± 1.31	84.63 ± 0.31	97.86 ± 1.46	83.72 ± 1.40	96.25 ± 0.25	<b>87.28 ± 3.50</b>	81.42 ± 11.55	9.50
MMLP CB	69.85 ± 1.51	67.46 ± 1.62	84.91 ± 0.45	70.17 ± 2.01	83.68 ± 0.32	95.23 ± 2.54	nan	nan	<b>86.81 ± 3.32</b>	83.57 ± 7.45	12.62
MMLP Classic	70.61 ± 7.44	70.96 ± 1.65	86.60 ± 0.40	70.70 ± 7.33	84.42 ± 0.28	99.91 ± 0.09	77.83 ± 1.63	95.24 ± 0.23	80.95 ± 0.54	<b>85.38 ± 8.02</b>	10.25
Transformer Classic	72.65 ± 1.15	70.70 ± 1.50	86.79 ± 0.34	71.96 ± 1.03	84.97 ± 0.27	<b>99.92 ± 0.09</b>	80.69 ± 1.55	96.18 ± 0.24	80.95 ± 0.46	<b>89.68 ± 7.31</b>	8.90

Table 9: Hypergraph model performance benchmarks. Test accuracy in % averaged over 15 splits. Training split: 30%.

Model	Cora	Citeseer	Pubmed	CORA-CA	DBLP-CA	Mushroom	NTU2012	ModelNet40	20Newsgroups	ZOO	avg. ranking
AllDeepSets	74.78 ± 1.02	69.10 ± 1.34	<b>88.01 ± 0.39</b>	79.69 ± 1.44	90.57 ± 0.20	<b>99.95 ± 0.06</b>	84.04 ± 1.39	96.49 ± 0.26	80.99 ± 0.41	87.04 ± 6.74	6.45
AllSetTransformer	<b>77.67 ± 0.92</b>	71.06 ± 1.00	87.62 ± 0.34	<b>82.14 ± 0.96</b>	<b>91.10 ± 0.18</b>	99.94 ± 0.09	<b>85.73 ± 1.38</b>	97.73 ± 0.21	81.05 ± 0.49	90.19 ± 6.18	<b>3.30</b>
UniGCNII	76.29 ± 1.05	71.38 ± 1.32	87.48 ± 0.35	<b>81.93 ± 1.09</b>	<b>90.97 ± 0.20</b>	99.88 ± 0.08	<b>85.59 ± 1.60</b>	<b>97.89 ± 0.16</b>	81.10 ± 0.44	88.33 ± 6.29	3.65
CEGAT	74.25 ± 1.24	69.75 ± 0.90	85.41 ± 0.44	75.24 ± 1.05	87.54 ± 0.23	96.86 ± 1.27	79.12 ± 1.60	91.89 ± 0.30	nan	42.87 ± 8.96	10.94
CEGCN	74.84 ± 1.35	69.17 ± 0.93	85.17 ± 0.41	74.83 ± 1.72	87.10 ± 0.25	95.08 ± 0.40	78.13 ± 1.35	89.34 ± 0.40	nan	48.70 ± 5.96	11.44
HCHA	<b>77.81 ± 1.07</b>	71.10 ± 1.11	84.97 ± 0.41	81.81 ± 1.08	90.85 ± 0.18	99.00 ± 0.47	84.34 ± 1.61	94.38 ± 0.28	80.78 ± 0.43	<b>90.65 ± 5.58</b>	6.30
HGNN	<b>77.81 ± 1.07</b>	70.88 ± 1.05	84.97 ± 0.41	81.78 ± 1.13	90.85 ± 0.16	99.00 ± 0.47	<b>84.40 ± 1.38</b>	94.38 ± 0.28	80.78 ± 0.43	<b>90.65 ± 5.58</b>	6.60
HNHN	74.85 ± 1.14	71.34 ± 1.03	86.34 ± 0.39	75.46 ± 1.02	86.33 ± 0.25	<b>99.95 ± 0.07</b>	<b>84.93 ± 1.49</b>	97.75 ± 0.20	81.10 ± 0.48	<b>85.37 ± 7.96</b>	5.50
HyperGCN	71.54 ± 1.26	63.82 ± 1.34	81.87 ± 0.56	74.44 ± 1.25	85.63 ± 2.89	69.44 ± 5.02	46.70 ± 4.01	45.28 ± 8.18	80.64 ± 0.48	55.46 ± 6.78	13.70
HAN	<b>78.60 ± 1.19</b>	<b>72.26 ± 0.93</b>	85.89 ± 0.44	<b>82.69 ± 0.77</b>	90.85 ± 0.19	91.47 ± 0.79	81.54 ± 1.44	93.79 ± 0.20	79.51 ± 0.58	79.18 ± 6.61	7.10
HAN minibatch	<b>78.84 ± 1.19</b>	<b>72.26 ± 0.93</b>	85.70 ± 0.81	79.81 ± 1.53	nan	93.59 ± 0.84	77.97 ± 1.63	nan	79.46 ± 1.10	45.74 ± 13.83	9.25
MultiRepMixer	77.43 ± 0.80	71.02 ± 1.19	84.07 ± 0.61	80.64 ± 0.94	89.55 ± 0.26	97.65 ± 1.11	<b>85.49 ± 1.60</b>	<b>98.04 ± 0.18</b>	85.97 ± 3.14	75.79 ± 10.03	6.80
MMLP CB	71.14 ± 1.09	70.21 ± 1.14	84.24 ± 0.63	71.14 ± 1.61	84.17 ± 0.24	97.46 ± 1.59	81.18 ± 1.79	96.10 ± 0.22	85.94 ± 5.83	79.58 ± 8.22	10.10
MMLP CB	67.43 ± 1.12	66.48 ± 1.20	84.32 ± 0.52	68.53 ± 1.25	83.00 ± 0.30	94.78 ± 2.67	nan	nan	<b>86.75 ± 3.67</b>	82.88 ± 7.48	11.88
MMLP Classic	66.14 ± 11.37	69.92 ± 1.32	85.86 ± 0.29	66.14 ± 11.37	83.96 ± 0.25	99.89 ± 0.11	75.08 ± 1.69	95.05 ± 0.31	80.82 ± 0.45	82.87 ± 7.37	10.80
Transformer Classic	70.41 ± 1.13	69.73 ± 1.33	86.05 ± 0.28	69.93 ± 0.92	84.57 ± 0.25	<b>99.93 ± 0.10</b>	78.20 ± 1.73	95.92 ± 0.20	80.87 ± 0.37	<b>86.85 ± 9.97</b>	9.25

Table 10: Hypergraph model performance benchmarks. Test accuracy in % averaged over 15 splits. Training split: 20%.

Model	Cora	Citeseer	Pubmed	CORA-CA	DBLP-CA	Mushroom	NTU2012	ModelNet40	20Newsgroups	ZOO	avg. ranking
AllDeepSets	72.56 ± 1.60	67.49 ± 1.57	<b>87.24 ± 0.36</b>	77.24 ± 1.52	89.91 ± 0.26	<b>99.92 ± 0.07</b>	80.71 ± 1.32	96.30 ± 0.24	80.59 ± 0.33	84.72 ± 7.95	6.25
AllSetTransformer	<b>75.69 ± 1.09</b>	69.39 ± 1.30	86.63 ± 0.40	<b>80.54 ± 0.94</b>	<b>90.72 ± 0.17</b>	<b>99.92 ± 0.07</b>	<b>82.58 ± 1.31</b>	97.48 ± 0.24	80.82 ± 0.28	85.61 ± 7.29	<b>3.35</b>
UniGCNII	74.11 ± 1.28	<b>70.51 ± 1.48</b>	<b>86.97 ± 0.41</b>	79.41 ± 1.23	90.47 ± 0.19	99.90 ± 0.06	<b>82.54 ± 1.60</b>	<b>97.83 ± 0.15</b>	80.88 ± 0.32	88.21 ± 5.55	3.50
CEGAT	71.86 ± 1.42	68.11 ± 1.34	84.03 ± 0.51	73.18 ± 1.32	86.98 ± 0.27	96.19 ± 1.38	76.14 ± 1.20	91.34 ± 0.31	nan	41.22 ± 6.16	10.67
CEGCN	73.25 ± 1.35	67.23 ± 1.39	83.47 ± 0.52	72.50 ± 1.44	86.29 ± 0.21	94.98 ± 0.31	75.55 ± 1.37	88.60 ± 0.41	nan	49.51 ± 6.31	11.56
HCHA	<b>76.04 ± 1.30</b>	69.90 ± 1.25	83.65 ± 0.37	<b>80.03 ± 0.87</b>	90.53 ± 0.17	99.03 ± 0.43	<b>81.48 ± 1.29</b>	94.31 ± 0.20	80.60 ± 0.29	<b>89.35 ± 5.89</b>	5.40
HGNN	<b>76.04 ± 1.30</b>	69.59 ± 1.22	83.65 ± 0.37	<b>80.02 ± 0.88</b>	90.51 ± 0.19	99.03 ± 0.43	<b>81.60 ± 1.24</b>	94.31 ± 0.20	80.60 ± 0.29	<b>89.35 ± 5.89</b>	5.60
HNHN	72.47 ± 1.06	69.44 ± 1.21	85.10 ± 0.47	73.16 ± 0.99	85.82 ± 0.21	<b>99.88 ± 0.10</b>	<b>81.56 ± 1.54</b>	97.61 ± 0.24	80.48 ± 0.32	82.60 ± 7.71	7.20
HyperGCN	68.59 ± 1.79	62.08 ± 1.28	81.57 ± 0.43	71.42 ± 1.27	85.45 ± 2.31	69.36 ± 5.10	44.01 ± 3.47	46.40 ± 8.41	80.38 ± 0.37	53.25 ± 8.74	

Table 11: Hypergraph model performance benchmarks. Test accuracy in % averaged over 15 splits. Training split: 10%.

Model	Cora	Citeseer	Pubmed	CORA-CA	DBLP-CA	Mushroom	NTU2012	ModelNet40	20Newsgroups	ZOO	avg. ranking
AllDeepSets	68.51 ± 1.64	64.50 ± 1.43	<b>85.55 ± 0.38</b>	73.67 ± 1.79	88.82 ± 0.25	<b>99.88 ± 0.08</b>	73.44 ± 1.91	95.96 ± 0.21	79.61 ± 0.36	76.81 ± 7.05	6.15
AllSetTransformer	<b>71.82 ± 1.18</b>	65.96 ± 1.48	84.71 ± 0.55	76.16 ± 1.36	<b>90.09 ± 0.18</b>	<b>99.86 ± 0.09</b>	<b>75.78 ± 1.96</b>	96.93 ± 0.21	80.18 ± 0.31	<b>75.22 ± 10.78</b>	4.05
UniGCNII	69.36 ± 1.63	66.41 ± 1.59	<b>85.51 ± 0.50</b>	75.84 ± 1.13	89.70 ± 0.25	<b>99.86 ± 0.09</b>	<b>74.86 ± 2.20</b>	<b>97.58 ± 0.18</b>	80.44 ± 0.26	<b>79.86 ± 9.97</b>	<b>3.65</b>
CEGAT	68.08 ± 1.65	64.15 ± 1.60	81.83 ± 0.43	69.04 ± 1.60	85.92 ± 0.23	96.01 ± 1.31	69.26 ± 2.27	90.17 ± 0.37	nan	39.20 ± 6.19	10.89
CEGCN	70.22 ± 1.62	62.68 ± 1.49	82.13 ± 0.44	67.45 ± 1.54	85.41 ± 0.26	94.85 ± 0.36	68.31 ± 2.08	87.28 ± 0.39	nan	49.20 ± 5.69	11.00
HCHA	<b>72.76 ± 1.82</b>	66.15 ± 1.27	82.41 ± 0.36	<b>76.97 ± 0.95</b>	<b>90.00 ± 0.19</b>	98.93 ± 0.41	<b>74.44 ± 2.31</b>	94.04 ± 0.21	80.23 ± 0.32	<b>79.78 ± 7.89</b>	4.95
HGNN	<b>72.76 ± 1.82</b>	65.69 ± 1.57	82.41 ± 0.36	<b>76.96 ± 1.10</b>	<b>90.00 ± 0.18</b>	98.93 ± 0.41	<b>74.53 ± 2.44</b>	94.04 ± 0.21	80.23 ± 0.32	<b>79.78 ± 7.89</b>	5.15
HNHN	67.43 ± 1.62	65.02 ± 1.40	82.33 ± 0.76	68.10 ± 1.67	84.74 ± 0.31	99.69 ± 0.18	73.82 ± 2.11	97.34 ± 0.25	80.00 ± 0.26	<b>73.12 ± 6.57</b>	7.80
HyperGCN	63.21 ± 1.95	57.81 ± 1.91	80.83 ± 0.46	65.58 ± 2.02	84.37 ± 1.73	67.56 ± 8.16	40.30 ± 3.67	45.92 ± 7.60	79.57 ± 0.38	51.96 ± 6.32	13.60
HAN	<b>72.08 ± 1.47</b>	<b>67.86 ± 1.46</b>	85.10 ± 0.43	<b>77.48 ± 1.22</b>	<b>90.02 ± 0.17</b>	91.67 ± 0.86	72.91 ± 1.88	93.52 ± 0.32	78.77 ± 0.49	70.94 ± 14.54	6.50
HAN minibatch	69.61 ± 6.86	<b>68.25 ± 1.15</b>	84.93 ± 0.65	<b>76.27 ± 1.54</b>	nan	nan	63.36 ± 2.66	nan	nan	43.62 ± 9.44	7.50
MultiRepMixer	<b>71.54 ± 1.37</b>	66.54 ± 1.44	81.40 ± 0.85	74.94 ± 1.25	88.50 ± 0.31	93.93 ± 2.80	<b>75.05 ± 1.94</b>	<b>97.50 ± 0.24</b>	<b>83.82 ± 3.17</b>	66.30 ± 7.66	6.80
MLP CB	62.42 ± 1.37	64.85 ± 1.30	81.43 ± 0.86	62.82 ± 1.80	82.02 ± 0.36	94.17 ± 2.92	68.80 ± 1.51	95.16 ± 0.26	<b>85.21 ± 3.81</b>	67.46 ± 9.14	10.10
MMLP CB	57.17 ± 1.86	59.40 ± 1.86	82.06 ± 0.59	59.03 ± 1.52	80.22 ± 0.35	91.88 ± 2.50	nan	nan	<b>85.03 ± 2.38</b>	69.95 ± 8.10	12.00
MLP Classic	38.64 ± 12.37	64.21 ± 1.53	83.56 ± 0.49	37.85 ± 11.79	81.88 ± 0.21	99.72 ± 0.15	63.39 ± 2.24	93.71 ± 0.38	79.63 ± 0.42	<b>72.17 ± 9.21</b>	10.80
Transformer Classic	61.45 ± 1.66	63.75 ± 1.39	83.86 ± 0.50	60.65 ± 1.87	82.40 ± 0.47	99.74 ± 0.20	65.14 ± 1.61	94.66 ± 0.42	79.61 ± 0.39	68.82 ± 8.32	10.25

Table 12: Split 20%

Model	AllSetTransformer	UniGCNII	HCHA	HNHN	HGNN	AllDeepSets	MultiSetMixer	HAN	Transformer Classic	MLP HP	MLP classic	CEGAT	CEGCN	MMLP HP	MLP	HyperGCN
0.1	3.75	3.35	4.85	7.45	5.05	5.85	6.700	6.80	9.320	10.100	10.090	10.670	11.000	11.880	12.05	13.70
0.2	3.35	3.50	5.50	7.20	5.70	6.25	6.700	7.25	9.270	10.300	10.500	11.000	11.890	12.000	12.70	14.10
0.3	3.30	3.65	6.40	5.50	6.70	6.55	6.900	7.60	8.680	10.400	10.270	11.280	11.780	12.120	13.00	14.20
0.4	3.15	3.55	6.50	5.30	6.50	6.40	6.700	8.45	8.360	9.800	9.770	11.000	12.170	12.880	12.80	14.00
0.5	2.85	4.15	6.95	5.05	7.05	6.10	6.270	8.60	8.500	9.640	9.910	11.330	12.000	11.890	12.90	14.30
avg	3.28	3.64	6.04	6.10	6.20	6.23	6.654	7.74	8.826	10.048	10.108	11.056	11.768	12.154	12.69	14.06

## G EXPERIMENT RESULTS

### G.1 EXPERIMENT 1: BENCHMARKING MODELS ACROSS MULTIPLE TRAINING PROPORTIONS SPLITS

### G.2 EXPERIMENT 3: CONNECTIVITY MODIFICATION

## H SAMPLING ANALYSIS

In this Section, we provide an analysis regarding the uniform sampling of the hyperedges in Step 1. We propose sampling  $X$  mini-batches of a certain size  $B$  at each iteration. At *step 1*, we sample  $B$  hyperedges from  $\mathcal{E}$ ; in *step 2*, for each hyperedge we sample a fixed number of nodes, that are randomly chosen among the ones belonging to that specific hyperedge. If the hyperedge does not contain enough samples, we use padding so that the size of the set of sampled nodes is increased to the desired value. By choosing to sample the nodes uniformly at random from the hyperedge, there is no guarantee that we will eventually sample all the nodes of each hyperedge. Indeed, sampling uniformly at random  $c$  items from a set of size  $n$ , the probability of not sampling our desired one is  $1 - \frac{c}{n}$ . The probability of having to wait for  $T$  independent trials before finding node  $x$  among the sampled nodes is described by the geometric distribution.

Namely, let  $x \in e$  and  $|e| = n$ , and assume the size of the considered mini-batch is  $c$ :

$$\mathbb{P}(\text{Sample node } x \text{ from hyperedge } e \text{ for the first time at epoch } T) = \left(1 - \frac{c}{n}\right)^{T-1} \frac{c}{n}. \quad (43)$$

It follows that

$$\mathbb{E}[\text{\# of epochs to wait before sampling node } x] = \frac{n}{c}.$$

Assume now that a node  $x$  belongs to  $k$  hypergraphs  $e_1, \dots, e_k$  of respective sizes  $n_1, \dots, n_k$ . The events  $\{\text{Node } x \text{ is sampled from hyperedge } e_i\}$  and  $\{\text{Node } x \text{ is sampled from hyperedge } e_j\}$  are independent if  $i \neq j$ . It follows that the random variable  $\{\text{\# of epochs to wait until we sample node } x \text{ from all the hyperedges } e_1, \dots, e_k\}$  is the maximum of  $k$  independent non-identically distributed geometric distributions. Denote by  $T_i$  the random variable that corresponds to the number of epochs we have to wait before sampling sample  $x$  from edge  $e_i$ . The exact distribution for the random variable  $T$ , that is, the number of epochs we have to wait until we sample node  $x$  from all hyperedges  $e_1, \dots, e_k$  at least once, is

$$\mathbb{P}(T \leq h) = \mathbb{P}\left(\max_{i=1, \dots, k} T_i \leq h\right) = \prod_{i=1}^k \mathbb{P}(T_i \leq h) = \prod_{i=1}^k \left(1 - p_i\right)^h$$

It follows that

Table 13: Drop connectivity benchmarks. Test accuracy in % averaged over 15 splits.

Model	Type	Cora	Citeseer	Pubmed	CORA-CA	DBLP-CA	Mushroom	NTU2012	ModelNet40	20NewsGroups	ZOO	avg. ranking	
AllDeepSets	Original	<b>77.11 ± 1.00</b>	70.67 ± 1.42	<b>89.04 ± 0.45</b>	<b>82.23 ± 1.46</b>	<b>91.34 ± 0.27</b>	99.96 ± 0.05	<b>86.49 ± 1.86</b>	96.70 ± 0.25	81.19 ± 0.49	89.10 ± 7.00	<b>2.85</b>	
	Random 25%	76.65 ± 1.03	70.83 ± 1.70	88.87 ± 0.47	80.39 ± 1.51	90.36 ± 0.28	99.91 ± 0.09	85.49 ± 1.74	96.85 ± 0.26	81.15 ± 0.52	88.72 ± 5.97	4.05	
	Random 50%	75.66 ± 1.18	70.70 ± 1.77	88.86 ± 0.41	77.97 ± 1.18	89.36 ± 0.25	<b>99.93 ± 0.05</b>	84.42 ± 1.75	<b>96.88 ± 0.27</b>	81.21 ± 0.39	84.49 ± 6.66	4.90	
	Random 75%	74.96 ± 1.08	70.46 ± 1.66	88.76 ± 0.45	76.09 ± 1.27	87.68 ± 0.30	99.53 ± 0.13	81.70 ± 1.57	96.84 ± 0.27	81.31 ± 0.50	81.15 ± 6.88	7.50	
	Retention 25%	<b>76.87 ± 0.98</b>	<b>70.96 ± 1.82</b>	88.94 ± 0.48	<b>81.63 ± 1.26</b>	90.93 ± 0.18	99.83 ± 0.09	<b>85.13 ± 2.05</b>	96.85 ± 0.26	81.09 ± 0.46	86.67 ± 7.26	3.65	
	Retention 50%	75.80 ± 1.06	70.44 ± 1.63	88.84 ± 0.40	80.50 ± 1.38	90.55 ± 0.21	99.91 ± 0.09	82.25 ± 2.21	96.42 ± 0.23	81.04 ± 0.45	69.61 ± 9.28	6.75	
	Retention 75%	75.52 ± 1.49	70.36 ± 1.71	88.78 ± 0.47	79.50 ± 1.09	89.48 ± 0.21	<b>99.97 ± 0.04</b>	78.85 ± 1.93	96.44 ± 0.27	<b>81.19 ± 0.45</b>	74.49 ± 9.97	6.85	
	Trimming 25%	74.12 ± 1.30	70.95 ± 1.92	88.77 ± 0.45	74.87 ± 1.32	86.39 ± 0.31	99.85 ± 0.15	77.47 ± 1.67	96.18 ± 0.28	<b>81.61 ± 0.47</b>	<b>89.23 ± 8.11</b>	7.10	
	Trimming 50%	75.24 ± 0.99	70.42 ± 1.62	88.87 ± 0.46	75.89 ± 1.53	87.14 ± 0.31	<b>99.93 ± 0.06</b>	82.76 ± 1.61	96.75 ± 0.23	81.47 ± 0.48	86.28 ± 8.73	6.15	
	Trimming 75%	76.03 ± 1.39	70.86 ± 1.48	88.83 ± 0.48	77.50 ± 1.52	88.64 ± 0.27	99.93 ± 0.09	84.74 ± 1.81	96.82 ± 0.20	81.20 ± 0.48	86.03 ± 8.48	5.20	
AlibiTransformer	Original	<b>79.54 ± 1.02</b>	72.52 ± 0.88	<b>88.74 ± 0.51</b>	<b>84.43 ± 1.14</b>	<b>91.61 ± 0.19</b>	99.95 ± 0.05	<b>88.22 ± 1.42</b>	<b>98.00 ± 0.12</b>	81.59 ± 0.59	91.03 ± 7.31	<b>1.95</b>	
	Random 25%	79.11 ± 0.99	<b>72.75 ± 1.14</b>	88.07 ± 0.47	82.36 ± 1.38	90.61 ± 0.29	99.94 ± 0.09	87.50 ± 1.36	<b>97.98 ± 0.17</b>	<b>81.70 ± 0.52</b>	89.87 ± 7.66	3.10	
	Random 50%	77.77 ± 1.34	72.21 ± 1.25	88.50 ± 0.45	79.73 ± 1.58	89.46 ± 0.27	99.96 ± 0.04	87.34 ± 1.55	97.83 ± 0.17	<b>81.55 ± 0.66</b>	89.49 ± 6.30	5.85	
	Random 75%	76.92 ± 1.20	72.40 ± 1.22	88.54 ± 0.47	77.88 ± 1.74	87.73 ± 0.32	99.76 ± 0.15	86.31 ± 1.34	97.52 ± 0.20	81.46 ± 0.62	87.69 ± 6.09	8.10	
	Retention 25%	79.19 ± 1.11	72.49 ± 0.86	88.73 ± 0.40	<b>83.58 ± 1.30</b>	91.18 ± 0.17	<b>99.93 ± 0.09</b>	87.21 ± 1.58	97.82 ± 0.17	81.63 ± 0.48	86.92 ± 7.18	4.10	
	Retention 50%	78.16 ± 0.98	72.55 ± 1.13	88.70 ± 0.37	82.90 ± 1.15	90.80 ± 0.22	99.89 ± 0.18	86.67 ± 1.64	97.36 ± 0.21	81.61 ± 0.49	88.08 ± 7.51	5.20	
	Retention 75%	77.38 ± 1.35	72.43 ± 0.98	88.71 ± 0.39	81.07 ± 1.20	89.83 ± 0.25	<b>99.97 ± 0.04</b>	85.58 ± 1.70	97.27 ± 0.22	81.58 ± 0.48	88.97 ± 6.91	5.80	
	Trimming 25%	75.83 ± 1.31	72.39 ± 1.50	88.40 ± 0.45	76.51 ± 1.35	86.38 ± 0.32	99.84 ± 0.13	86.88 ± 1.66	97.10 ± 0.24	81.55 ± 0.55	<b>93.08 ± 7.79</b>	8.05	
	Trimming 50%	77.37 ± 1.17	72.32 ± 1.30	88.49 ± 0.40	77.41 ± 1.73	87.03 ± 0.27	99.91 ± 0.12	86.86 ± 1.53	97.95 ± 0.21	81.45 ± 0.50	87.74 ± 8.53	7.50	
	Trimming 75%	78.15 ± 1.11	72.07 ± 1.00	88.48 ± 0.39	78.91 ± 1.54	88.55 ± 0.26	99.92 ± 0.09	87.68 ± 1.56	<b>97.90 ± 0.23</b>	81.41 ± 0.61	91.02 ± 7.17	5.35	
CEGAT	Original	<b>76.53 ± 1.58</b>	71.58 ± 1.11	87.11 ± 0.49	<b>77.50 ± 1.51</b>	<b>88.74 ± 0.31</b>	96.81 ± 1.41	82.27 ± 1.60	92.79 ± 0.44	nan	nan	4.62 ± 9.18	5.17
	Random 25%	75.88 ± 1.53	71.81 ± 1.05	87.03 ± 0.47	<b>78.00 ± 1.68</b>	87.58 ± 0.35	94.56 ± 2.09	82.03 ± 1.47	93.14 ± 0.34	nan	nan	46.03 ± 9.01	5.94
	Random 50%	75.34 ± 1.52	71.86 ± 1.22	86.91 ± 0.48	76.92 ± 1.00	86.81 ± 0.32	95.14 ± 2.00	81.73 ± 1.44	93.62 ± 0.35	nan	nan	47.69 ± 6.91	6.89
	Random 75%	75.26 ± 1.45	72.17 ± 1.59	87.02 ± 0.47	76.37 ± 1.26	85.79 ± 0.35	96.90 ± 1.40	82.66 ± 1.39	94.54 ± 0.43	nan	nan	59.87 ± 8.55	5.22
	Retention 25%	75.96 ± 1.16	71.39 ± 1.33	87.13 ± 0.50	77.35 ± 1.52	<b>88.48 ± 0.30</b>	96.65 ± 1.49	80.39 ± 1.53	93.20 ± 0.45	nan	nan	45.26 ± 9.40	6.39
	Retention 50%	75.36 ± 1.30	71.56 ± 1.27	87.16 ± 0.53	77.35 ± 1.52	88.14 ± 0.31	96.73 ± 1.59	80.56 ± 2.16	93.86 ± 0.41	nan	nan	45.38 ± 9.97	6.00
	Retention 75%	76.12 ± 1.58	72.06 ± 1.42	86.94 ± 0.56	77.20 ± 1.47	87.54 ± 0.28	94.04 ± 0.48	79.20 ± 1.42	90.59 ± 0.59	nan	nan	45.38 ± 9.97	6.00
	Trimming 25%	75.40 ± 1.45	<b>72.67 ± 1.76</b>	<b>87.68 ± 0.52</b>	76.14 ± 1.10	85.32 ± 0.42	<b>99.72 ± 0.10</b>	<b>84.94 ± 1.57</b>	94.42 ± 0.33	nan	nan	<b>89.23 ± 7.38</b>	<b>3.67</b>
	Trimming 50%	75.90 ± 1.48	72.15 ± 1.62	87.41 ± 0.51	76.09 ± 1.65	85.69 ± 0.40	<b>99.80 ± 0.12</b>	82.04 ± 1.32	93.22 ± 0.38	nan	nan	67.05 ± 7.87	4.44
	Trimming 75%	76.19 ± 1.68	71.82 ± 1.32	87.03 ± 0.56	76.04 ± 0.95	86.18 ± 0.38	99.31 ± 0.24	81.74 ± 1.48	92.79 ± 0.33	nan	nan	53.33 ± 6.60	6.22
CEGCN	Original	<b>77.03 ± 1.31</b>	70.87 ± 1.19	87.01 ± 0.62	<b>77.55 ± 1.65</b>	<b>88.12 ± 0.25</b>	94.91 ± 0.44	80.90 ± 1.74	90.04 ± 0.47	nan	nan	49.23 ± 6.81	4.61
	Random 25%	76.08 ± 1.55	71.35 ± 1.44	86.89 ± 0.59	76.51 ± 1.53	87.01 ± 0.39	93.11 ± 0.46	80.68 ± 1.86	90.36 ± 0.46	nan	nan	47.74 ± 6.22	6.22
	Random 50%	75.55 ± 1.63	71.42 ± 1.60	86.70 ± 0.48	75.27 ± 1.22	86.24 ± 0.35	93.28 ± 0.61	80.63 ± 1.78	90.69 ± 0.54	nan	nan	56.92 ± 7.24	6.33
	Random 75%	75.34 ± 1.62	71.73 ± 1.90	86.97 ± 0.51	74.53 ± 1.56	85.36 ± 0.26	93.01 ± 0.45	80.56 ± 1.76	<b>91.91 ± 0.54</b>	nan	nan	63.20 ± 5.59	6.33
	Retention 25%	76.82 ± 1.58	70.83 ± 1.42	86.94 ± 0.56	76.98 ± 1.53	<b>87.90 ± 0.29</b>	94.04 ± 0.48	80.90 ± 1.82	90.59 ± 0.59	nan	nan	49.87 ± 7.59	5.06
	Retention 50%	75.43 ± 1.28	70.83 ± 1.52	86.95 ± 0.54	76.87 ± 1.49	87.58 ± 0.28	94.97 ± 0.40	78.53 ± 1.90	90.09 ± 0.56	nan	nan	45.77 ± 6.88	6.89
	Retention 75%	75.53 ± 1.25	71.72 ± 1.42	87.11 ± 0.53	76.36 ± 1.42	87.03 ± 0.28	94.74 ± 0.39	79.82 ± 1.41	<b>92.29 ± 0.46</b>	nan	nan	40.38 ± 5.42	5.84
	Trimming 25%	75.58 ± 1.56	<b>72.26 ± 1.52</b>	<b>87.36 ± 0.51</b>	74.84 ± 1.31	84.97 ± 0.31	<b>99.60 ± 0.11</b>	<b>83.10 ± 1.69</b>	91.85 ± 0.42	nan	nan	<b>87.69 ± 7.31</b>	<b>3.44</b>
	Trimming 50%	76.57 ± 1.47	71.81 ± 1.44	87.07 ± 0.55	74.66 ± 1.68	85.24 ± 0.33	<b>99.54 ± 0.18</b>	80.72 ± 1.64	90.64 ± 0.54	nan	nan	71.28 ± 6.60	4.00
	Trimming 75%	76.53 ± 1.50	71.45 ± 1.45	86.75 ± 0.54	74.56 ± 1.32	85.56 ± 0.33	99.14 ± 0.23	80.38 ± 1.91	90.06 ± 0.37	nan	nan	58.46 ± 7.17	6.22
HCIA	Original	<b>79.53 ± 1.33</b>	<b>72.57 ± 1.06</b>	<b>86.97 ± 0.55</b>	<b>83.53 ± 1.12</b>	<b>91.21 ± 0.28</b>	98.94 ± 0.54	<b>86.60 ± 1.96</b>	94.50 ± 0.33	<b>80.75 ± 0.53</b>	89.23 ± 6.81	<b>2.40</b>	
	Random 25%	78.74 ± 1.30	72.53 ± 1.28	86.84 ± 0.56	81.98 ± 1.34	90.09 ± 0.35	98.55 ± 0.55	85.94 ± 1.76	94.78 ± 0.28	80.16 ± 0.46	89.10 ± 6.71	4.30	
	Random 50%	77.65 ± 1.46	72.11 ± 1.42	86.67 ± 0.48	79.23 ± 1.41	88.88 ± 0.35	98.61 ± 0.48	83.32 ± 1.75	95.17 ± 0.28	79.68 ± 0.50	87.56 ± 6.97	7.60	
	Random 75%	76.56 ± 1.60	72.23 ± 1.33	86.72 ± 0.56	77.11 ± 1.28	87.07 ± 0.34	98.59 ± 0.76	84.88 ± 1.44	<b>95.57 ± 0.34</b>	79.49 ± 0.43	82.18 ± 6.58	7.30	
	Retention 25%	79.09 ± 1.25	72.29 ± 1.17	86.95 ± 0.52	<b>83.06 ± 1.09</b>	90.63 ± 0.25	98.82 ± 0.50	85.56 ± 1.66	94.73 ± 0.34	<b>80.27 ± 0.44</b>	<b>86.03 ± 5.20</b>	3.85	
	Retention 50%	77.77 ± 1.38	72.20 ± 1.20	86.82 ± 0.48	82.16 ± 1.27	90.17 ± 0.29	98.22 ± 0.28	84.80 ± 1.79	94.54 ± 0.22	79.96 ± 0.44	77.77 ± 6.86	6.70	
	Retention 75%	77.05 ± 1.53	72.37 ± 1.20	86.79 ± 0.47	80.79 ± 0.95	88.97 ± 0.24	97.62 ± 0.30	84.35 ± 1.65	95.21 ± 0.30	79.40 ± 0.52	84.36 ± 6.77	6.70	
	Trimming 25%	75.68 ± 1.21	72.15 ± 1.72	86.83 ± 0.47	75.94 ± 1.35	85.85 ± 0.40	<b>99.87 ± 0.11</b>	<b>85.60 ± 1.92</b>	95.02 ± 0.26	<b>80.66 ± 0.56</b>	<b>91.92 ± 7.10</b>	5.50	
	Trimming 50%	77.76 ± 1.28	72.10 ± 1.49	86.96 ± 0.48	77.26 ± 1.17	86.57 ± 0.36	<b>99.84 ± 0.11</b>	84.58 ± 1.37	94.73 ± 0.28	80.18 ± 0.60	83.08 ± 8.72	6.45	
	Trimming 75%	78.38 ± 1.30	72.22 ± 1.12	86.81 ± 0.53	78.82 ± 0.95	88.09 ± 0.27	99.73 ± 0.18	<b>86.05 ± 1.60</b>	94.61 ± 0.27	80.02 ± 0.57	<b>89.36 ± 8.49</b>	5.20	
HCNN	Original	<b>79.53 ± 1.33</b>	<b>72.24 ± 1.08</b>	<b>86.97 ± 0.55</b>	<b>83.45 ± 1.22</b>	<b>91.26 ± 0.26</b>	98.94 ± 0.54	<b>86.71 ± 1.48</b>	94.50 ± 0.33	<b>80.75 ± 0.52</b>	89.23 ± 6.81	<b>2.50</b>	
	Random 25%	78.74 ± 1.30	72.15 ± 1.36	86.84 ± 0.56	81.94 ± 1.31	90.11 ± 0.34	98.55 ± 0.55	85.82 ± 1.65	94.78 ± 0.28	80.16 ± 0.43	89.10 ± 6.71	4.70	
	Random 50%	77.65 ± 1.46	72.20 ± 1.62	86.67 ± 0.48	79.20 ± 1.48	88.84 ± 0.42	98.61 ± 0.48	85.59 ± 1.49	95.17 ± 0.28	79.68 ± 0.50	87.56 ± 6.97	5.95	
	Random 75%	76.56 ± 1.60	72.16 ± 1.56	86.72 ± 0.56	77.03 ± 1.37	86.95 ± 0.34	98.59 ± 0.76	85.12 ± 1.27	<b>95.57 ± 0.34</b>	79.50 ± 0.42	82.18 ± 6.58	7.30	
	Retention 25%	79.09 ± 1.25	72.13 ± 1.17	86.95 ± 0.52	<b>83.11 ± 1.09</b>	90.66 ± 0.23	98.82 ± 0.50	<b>85.33 ± 1.52</b>	94.73 ± 0.34	80.23 ± 0.44	86.03 ± 5.20	4.25	
	Retention 50%	77.77 ± 1.38	72.20 ± 1.32	86.82 ± 0.48	82.20 ± 1.29	90.21 ± 0.27	98.22 ± 0.28	84.51 ± 1.77	94.54 ± 0.22	79.93 ± 0.46	75.77 ± 6.86	6.45	
	Retention 75%	77.05 ± 1.53	<b>72.35 ± 1.40</b>	86.79 ± 0.47	80.88 ± 0.93	89.02 ± 0.23	<b>97.62 ± 0.30</b>	84.19 ± 1.49	95.21 ± 0.30	79.36 ± 0.54	84.36 ± 6.77	6.60	
	Trimming 25%	77.27 ± 1.01	72.69 ± 1.31	87.93 ± 0.52	78.68 ± 0.96	89.26 ± 0.28	<b>99.84 ± 0.11</b>	<b>85.89 ± 1.67</b>	<b>90.66 ± 0.47</b>	<b>81.92 ± 7.10</b>	<b>89.36 ± 8.49</b>	5.55	
	Trimming 50%	77.76 ± 1.28	71.91 ± 1.50	86.96 ± 0.48	77.29 ± 1.18	86.48 ± 0.34	<b>99.84 ± 0.11</b>	84.67 ± 1.43	94.73 ± 0.28	80.18 ± 0.60	83.08 ± 8.72	6.30	
	Trimming 75%	78.38 ± 1.30	72.07 ± 1.25	86.81 ± 0.53	78.78 ± 1.04	87.99 ± 0.34	99.73 ± 0.18	<b>86.00 ± 1.55</b>	94				

Table 14: Adjust connectivity. Test accuracy in % averaged over 15 splits.

Model	Type	Cora	Citeseer	Pubmed	CORA-CA	DBLP-CA	Mushroom	NTU2012	ModelNet40	20NewsGroups	ZOO	avg. ranking
AllDeepSets	Label Based	<b>82.24 ± 1.12</b>	<b>75.65 ± 1.57</b>	<b>90.49 ± 0.40</b>	<b>91.12 ± 0.92</b>	<b>96.59 ± 0.17</b>	<b>99.96 ± 0.04</b>	<b>93.13 ± 1.29</b>	<b>99.52 ± 0.11</b>	<b>99.79 ± 0.13</b>	<b>91.54 ± 7.24</b>	<b>1.05</b>
	k-means	75.20 ± 1.11	70.87 ± 1.54	88.96 ± 0.48	79.59 ± 1.42	89.75 ± 0.25	<b>99.94 ± 0.09</b>	84.23 ± 1.50	97.17 ± 0.13	81.18 ± 0.54	86.92 ± 7.73	2.80
	Original	77.11 ± 1.00	70.67 ± 1.42	89.04 ± 0.45	82.23 ± 1.46	91.34 ± 0.27	<b>99.96 ± 0.05</b>	86.49 ± 1.86	96.70 ± 0.25	81.19 ± 0.49	89.10 ± 7.00	2.15
AllSetTransformer	Label Based	<b>83.43 ± 1.36</b>	<b>76.45 ± 1.43</b>	<b>90.19 ± 0.42</b>	<b>91.71 ± 0.89</b>	<b>96.75 ± 0.16</b>	<b>99.96 ± 0.05</b>	<b>94.81 ± 1.04</b>	<b>99.68 ± 0.09</b>	<b>99.93 ± 0.03</b>	<b>94.10 ± 6.91</b>	<b>1.05</b>
	k-means	77.14 ± 1.46	72.83 ± 1.07	88.60 ± 0.41	81.92 ± 1.35	89.79 ± 0.30	<b>99.96 ± 0.06</b>	87.95 ± 1.28	97.29 ± 0.20	81.58 ± 0.55	88.72 ± 7.69	2.75
	Original	79.54 ± 1.02	72.52 ± 0.88	88.74 ± 0.51	84.43 ± 1.14	91.61 ± 0.19	<b>99.95 ± 0.05</b>	88.22 ± 1.42	98.00 ± 0.12	81.59 ± 0.59	91.03 ± 7.31	2.20
UniGCNII	Label Based	<b>82.12 ± 1.11</b>	<b>75.23 ± 1.64</b>	<b>89.18 ± 0.50</b>	<b>89.80 ± 0.95</b>	<b>94.78 ± 0.13</b>	<b>99.93 ± 0.07</b>	<b>92.87 ± 1.32</b>	<b>99.31 ± 0.10</b>	<b>99.70 ± 0.10</b>	<b>94.74 ± 6.35</b>	<b>1.00</b>
	k-means	76.49 ± 1.01	72.73 ± 1.50	88.02 ± 0.48	81.13 ± 1.41	90.13 ± 0.26	<b>99.88 ± 0.07</b>	88.05 ± 1.78	97.10 ± 0.21	81.06 ± 0.48	89.23 ± 7.52	3.00
	Original	78.46 ± 1.14	73.05 ± 1.48	88.07 ± 0.47	83.92 ± 1.02	91.56 ± 0.18	<b>99.89 ± 0.07</b>	88.24 ± 1.56	97.84 ± 0.16	81.16 ± 0.49	89.61 ± 8.09	2.00
CEGAT	Label Based	<b>83.05 ± 1.08</b>	<b>77.82 ± 1.59</b>	<b>90.25 ± 0.39</b>	<b>91.42 ± 0.88</b>	<b>96.25 ± 0.13</b>	<b>99.91 ± 0.07</b>	<b>94.23 ± 0.77</b>	<b>99.26 ± 0.14</b>	OOM	<b>93.85 ± 7.39</b>	<b>1.00</b>
	k-means	75.45 ± 1.54	72.57 ± 1.12	87.32 ± 0.47	77.11 ± 1.51	87.27 ± 0.29	97.66 ± 0.72	85.48 ± 1.66	96.39 ± 0.26	OOM	68.08 ± 8.28	2.33
	Original	76.53 ± 1.58	71.58 ± 1.11	87.11 ± 0.49	77.50 ± 1.51	88.74 ± 0.31	96.81 ± 1.41	82.27 ± 1.60	92.79 ± 0.44	OOM	44.62 ± 9.18	2.67
CEGCN	Label Based	<b>83.70 ± 1.02</b>	<b>77.50 ± 1.53</b>	<b>90.08 ± 0.42</b>	<b>91.28 ± 0.97</b>	<b>96.68 ± 0.14</b>	<b>99.95 ± 0.05</b>	<b>94.03 ± 1.24</b>	<b>99.30 ± 0.14</b>	OOM	<b>95.00 ± 7.08</b>	<b>1.00</b>
	k-means	75.89 ± 1.53	72.07 ± 1.18	87.13 ± 0.51	76.43 ± 1.41	86.76 ± 0.24	94.84 ± 0.47	85.34 ± 1.71	95.77 ± 0.31	OOM	73.72 ± 7.89	2.44
	Original	77.03 ± 1.31	70.87 ± 1.19	87.01 ± 0.62	77.55 ± 1.65	88.12 ± 0.25	94.91 ± 0.44	80.90 ± 1.74	90.04 ± 0.47	OOM	49.23 ± 6.81	2.56
HCHA	Label Based	<b>84.06 ± 1.08</b>	<b>77.12 ± 1.37</b>	<b>88.81 ± 0.43</b>	<b>92.77 ± 0.73</b>	<b>96.70 ± 0.12</b>	<b>99.96 ± 0.06</b>	<b>95.21 ± 1.27</b>	<b>99.67 ± 0.09</b>	<b>99.93 ± 0.04</b>	<b>94.61 ± 6.97</b>	<b>1.00</b>
	k-means	77.51 ± 1.41	72.62 ± 1.33	86.89 ± 0.48	81.19 ± 1.31	89.42 ± 0.29	99.56 ± 0.27	87.62 ± 1.33	96.98 ± 0.15	80.58 ± 0.57	84.10 ± 9.83	2.60
	Original	79.53 ± 1.33	72.57 ± 1.06	86.97 ± 0.55	83.53 ± 1.12	91.21 ± 0.28	98.94 ± 0.54	86.60 ± 1.96	94.50 ± 0.33	80.75 ± 0.53	89.23 ± 6.81	2.40
HGNN	Label Based	<b>84.06 ± 1.08</b>	<b>77.11 ± 1.47</b>	<b>88.81 ± 0.43</b>	<b>92.86 ± 0.65</b>	<b>96.70 ± 0.11</b>	<b>99.96 ± 0.06</b>	<b>95.34 ± 1.07</b>	<b>99.67 ± 0.09</b>	<b>99.93 ± 0.04</b>	<b>94.61 ± 6.97</b>	<b>1.00</b>
	k-means	77.51 ± 1.41	72.41 ± 1.55	86.89 ± 0.48	81.19 ± 1.38	89.42 ± 0.27	99.56 ± 0.27	87.52 ± 1.51	96.98 ± 0.15	80.58 ± 0.57	84.10 ± 9.83	2.60
	Original	79.53 ± 1.33	72.24 ± 1.08	86.97 ± 0.55	83.45 ± 1.22	91.26 ± 0.26	98.94 ± 0.54	86.71 ± 1.48	94.50 ± 0.33	80.75 ± 0.52	89.23 ± 6.81	2.40
HyperGCN	Label Based	<b>72.88 ± 1.23</b>	<b>66.10 ± 1.79</b>	<b>82.18 ± 0.62</b>	<b>76.20 ± 1.50</b>	<b>84.86 ± 0.39</b>	<b>69.68 ± 4.90</b>	<b>43.37 ± 4.65</b>	<b>47.19 ± 6.42</b>	<b>82.14 ± 0.43</b>	<b>53.97 ± 8.24</b>	<b>1.50</b>
	k-means	45.76 ± 1.97	49.96 ± 1.68	77.97 ± 0.75	47.63 ± 1.36	40.87 ± 4.04	69.53 ± 4.91	32.21 ± 2.57	41.96 ± 2.40	80.85 ± 0.46	53.46 ± 8.65	2.70
	Original	<b>74.78 ± 1.11</b>	66.06 ± 1.58	<b>82.32 ± 0.62</b>	<b>77.48 ± 1.14</b>	<b>86.07 ± 3.32</b>	69.51 ± 4.98	<b>47.65 ± 5.01</b>	46.10 ± 7.95	80.84 ± 0.49	51.54 ± 9.88	1.80
MultiSetMixer	Label Based	<b>82.59 ± 0.94</b>	<b>76.14 ± 1.03</b>	<b>88.35 ± 0.59</b>	<b>90.86 ± 0.67</b>	<b>96.38 ± 0.22</b>	<b>99.97 ± 0.04</b>	<b>93.72 ± 1.00</b>	<b>99.56 ± 0.12</b>	<b>99.85 ± 0.06</b>	<b>91.79 ± 6.90</b>	<b>1.05</b>
	kmeans based	76.78 ± 1.15	73.10 ± 1.18	85.84 ± 0.59	80.06 ± 1.45	88.54 ± 0.27	<b>99.97 ± 0.05</b>	87.75 ± 1.09	96.94 ± 0.26	81.14 ± 0.47	85.41 ± 6.77	2.55
	Original	79.38 ± 1.08	72.79 ± 1.12	85.71 ± 0.49	82.62 ± 1.20	89.87 ± 0.29	95.85 ± 3.21	88.73 ± 1.29	98.15 ± 0.19	87.83 ± 2.68	78.67 ± 9.08	2.40
MLP CB	Label Based	<b>74.54 ± 1.51</b>	<b>72.41 ± 1.47</b>	<b>86.02 ± 0.50</b>	<b>74.71 ± 1.16</b>	<b>84.88 ± 0.38</b>	<b>99.97 ± 0.06</b>	<b>85.94 ± 1.59</b>	<b>96.38 ± 0.32</b>	81.09 ± 0.52	<b>87.56 ± 7.33</b>	<b>1.50</b>
	k-means	74.53 ± 1.34	72.23 ± 1.55	85.99 ± 0.39	74.46 ± 1.32	84.78 ± 0.35	<b>99.97 ± 0.04</b>	<b>86.16 ± 1.54</b>	96.31 ± 0.27	81.09 ± 0.55	87.44 ± 7.25	2.10
	Original	74.06 ± 1.26	71.93 ± 1.53	85.83 ± 0.51	74.39 ± 1.40	<b>84.91 ± 0.44</b>	96.83 ± 2.18	<b>85.43 ± 1.51</b>	<b>96.41 ± 0.32</b>	<b>86.13 ± 2.82</b>	81.61 ± 10.98	2.40
MMLP CB	Label Based	<b>74.39 ± 1.52</b>	<b>72.09 ± 1.68</b>	84.94 ± 0.61	<b>74.61 ± 1.42</b>	83.68 ± 0.37	99.95 ± 0.07	NA	NA	81.31 ± 0.51	<b>87.18 ± 8.10</b>	<b>1.62</b>
	k-means	74.18 ± 1.54	71.21 ± 1.41	<b>85.51 ± 0.47</b>	74.49 ± 1.44	82.44 ± 0.41	<b>99.97 ± 0.05</b>	NA	NA	81.23 ± 0.53	85.90 ± 8.65	2.00
	Original	71.05 ± 2.03	69.26 ± 1.91	<b>85.20 ± 0.54</b>	71.16 ± 2.17	<b>84.08 ± 0.42</b>	95.71 ± 2.42	NA	NA	<b>85.04 ± 4.04</b>	83.89 ± 9.52	2.38

Table 15: K-means

Type	20NewsGroups	ModelNet40	Mushroom	NTU2012	Citeseer	CORA-CA	DBLP-CA	Cora	Pubmed	ZOO
MPL - max	-6.9	-2.84	-0.06	-9.03	-1.62	-11.16	-6.84	-7.46	-1.91	-5.9
MPL - max (init_models)	-0.66	-2.69	-0.06	-8.58	-1.62	-11.16	-6.84	-7.46	-1.91	-5.9
MPL_HP - max	-1.7	-1.74	-3.14	-3.3	-1.76	-10.04	-6.7	-6.67	-3.21	-9.42
MPL_HP - max (init_models)	4.54	-1.59	-3.14	-2.85	-1.76	-10.04	-6.7	-6.67	-3.21	-9.42
Smallest gap	4.54	-1.59	-0.06	-2.85	-1.62	-10.04	-6.7	-6.67	-1.91	-5.9

(1985), so that

$$\mathbb{E} \left( \max_{i=1, \dots, k} T_i \right) \tag{46}$$

$$\leq \max_{i=1, \dots, k} \mathbb{E} (T_i) + \sqrt{\frac{k-1}{k} \sum_{i=1}^k \mathbb{V} (T_i)} = \max_{i=1, \dots, k} \frac{n}{c} + \sqrt{\frac{k-1}{k} k \left[ \frac{n}{c} \left( 1 - \frac{n}{c} \right) \right]} \tag{47}$$

$$= \frac{n}{c} + \sqrt{k-1 \left[ \frac{n}{c} \left( 1 - \frac{n}{c} \right) \right]} \tag{48}$$

**Probability that a specific node is not sampled in one epoch** Let  $v$  be a node and let  $d_v$  be its degree. In one epoch, we “see” all hyperedges but, of course, not necessarily all their nodes. It holds that

$$\mathbb{P} (\text{node } v \text{ is sampled in epoch } T) = 1 - \mathbb{P} (\text{node } v \text{ is not sampled in epoch } T) \tag{49}$$

We can write the event

$$\{ \text{node } v \text{ is not sampled in epoch } T \} = \cap_{e \text{ s.t. } v \in e} \{ \text{node } v \text{ is not sampled in } e \}.$$

It follows that

$$\mathbb{P} (\text{node } v \text{ is sampled in epoch } T) = \max \left\{ 1 - \prod_{i=1}^{d_v} \frac{c}{|e_i| - 1}, \mathbb{1}_{\min_{i=1, \dots, d_v} |e_i| < c} \right\} \tag{50}$$

Indeed, if any of the edges  $v$  belongs to has a size smaller than the batch size for nodes ( $c$ ), the node is for sure seen in the first epoch.

## I NODE HOMOPHILY

In this Section, we report the node homophily plots for the datasets not illustrated in Figure 1. For each dataset, we choose to illustrate 3 different levels of node homophily, respectively 0, 1 and 10— level homophily, using Equation 2 at  $t = 0, 1$  and 10 (left, middle, and right plots respectively). Horizontal lines depict class mean homophily, with numbers above indicating the number of visualized points per class.

I.1 FIGURE - NODE HOMOPHILY

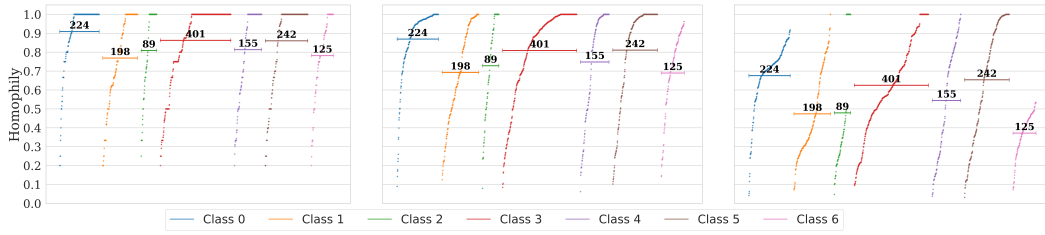


Figure 6: Node Homophily Distribution Scores for Cora

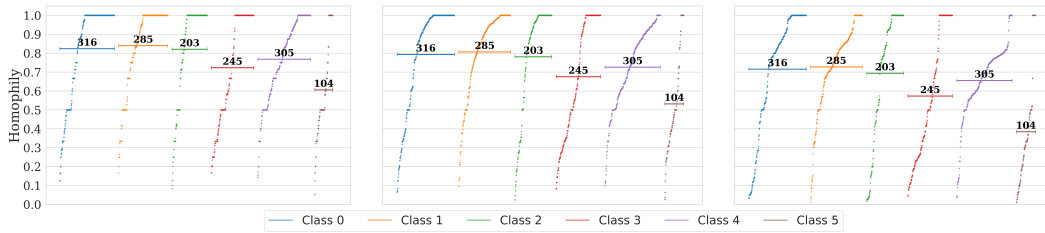


Figure 7: Node Homophily Distribution Scores for Citeseer

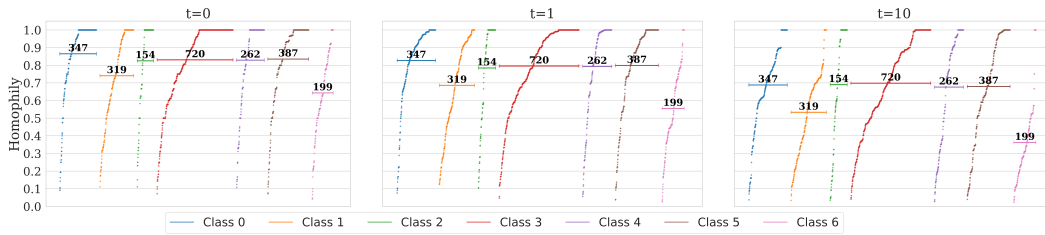


Figure 8: Node Homophily Distribution Scores for CORA-CA

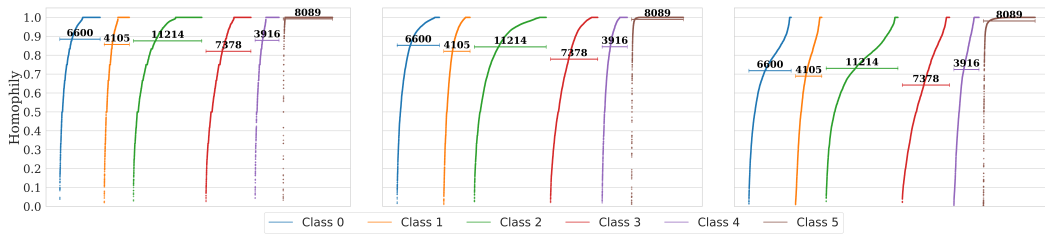


Figure 9: Node Homophily Distribution Scores for DBLP-CA

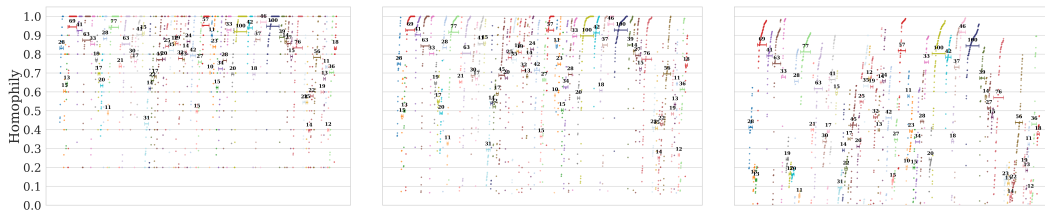


Figure 10: Node Homophily Distribution Scores for NTU2012

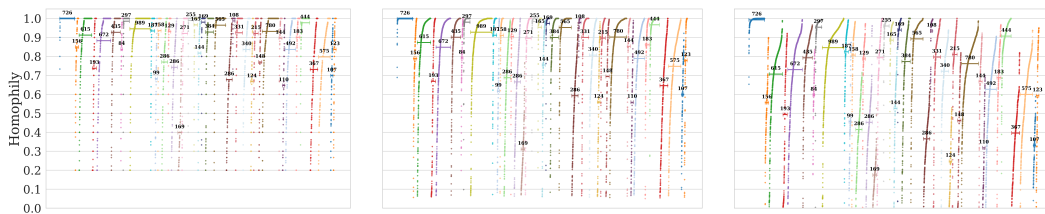


Figure 11: Node Homophily Distribution Scores for ModelNet40



Figure 12: Node Homophily Distribution Scores for Mushroom

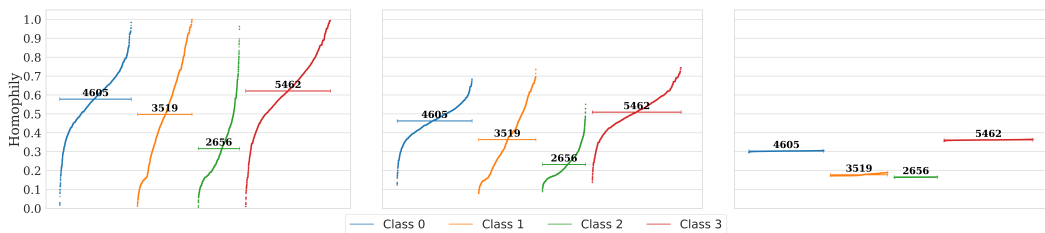


Figure 13: Node Homophily Distribution Scores for 20NewsW100

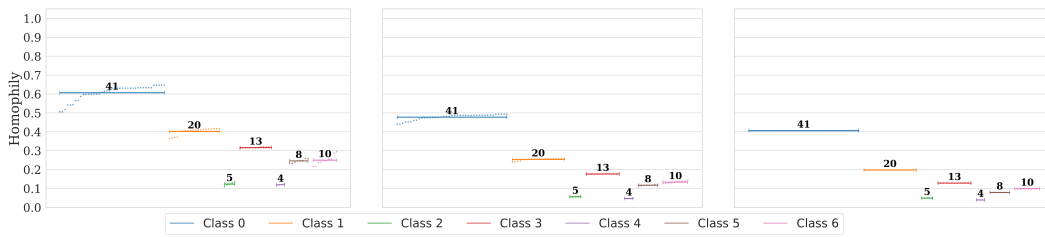


Figure 14: Node Homophily Distribution Scores for ZOO

---

## J FURTHER DETAILS ON K-UNIFORM HOMOPHILY MEASURE

**Hyperedge homophily** Veldt et al. (2023) defines the group homophily measure for  $k$ -uniform hypergraphs as  $G_k = (\mathcal{V}, \mathcal{E})$ . The type  $t$ -affinity score for each  $t \in \{1, \dots, k\}$ , indicates the likelihood of a node belonging to class  $c$  participating in groups in which exactly  $t$  group members also belong to class  $c$  and defined as in equation 51.  $d_t(v)$  is the number of hyperedges that  $v$  belongs to with exactly  $t$  members from class  $c$ . The authors also consider a standard baseline score  $b_t(c)$ , equation 52, that measures the probability that a class- $c$  node is in the group where  $t$  members are from class  $c$ , given that the other  $k - 1$  nodes were chosen uniformly at random.

$$\eta_t(c) = \frac{\sum_{v: y_v=c} d_t(v)}{\sum_{v: y_v=c} d_v}, \quad (51) \quad b_t(c) = \frac{\binom{n_c-1}{t-1} \binom{n-n_c}{k-t}}{\binom{n-1}{k-1}} \quad (52)$$

$n_c$  is the number of nodes in class  $c$  and  $n$  is the total number of nodes in the hypergraph. The  $k$ -uniform hypergraph homophily measure can be expressed as a ratio of affinity and baseline scores, with a ratio value of 1 indicating that the group is formed uniformly at random, while any other number indicates that group interactions are either overexpressed or underexpressed for class  $c$ .

They suggest three possible ways for extending the concept of homophily to the hypergraph context. The first one is the *simple* homophily and it means that  $\eta_t(c) > b_t(c)$  for  $t = k$  and check whether a class has a higher-than-baseline affinity for group interactions that only involve members of their class. The second one is *order- $j$  majority* homophily that is obtained when the top  $j$  affinity scores for one class are higher than the baseline, i.e.  $\eta_{k-j+1}(c) > b_{k-j+1}(c), \dots, \eta_k(c) > b_k(c)$ . The last one they consider is *order- $j$  monotonic* homophily, which corresponds to the case when top  $j$  ratio scores are increasing monotonic, i.e.  $\eta_k(c)/b_k(c) > \eta_{k-1}(c)/b_{k-1}(c) > \dots > \eta_{k-j+1}(c) > b_{k-j+1}(c)$ .

Finally, considering that the value  $\eta_t(c) - b_t(c)$  is the *bias* of class  $c$  for type  $t$ , they introduce a *type- $t$  normalized bias* score that normalizes the maximum possible bias, hence the obtained metric is bounded in  $[0, 1]$  and it is computed as:

$$f_t(c) = \begin{cases} \frac{\eta_t(c) - b_t(c)}{1 - b_t(c)} & \text{if } \eta_t(c) \geq b_t(c) \\ \frac{\eta_t(c) - b_t(c)}{b_t(c)} & \text{if } \eta_t(c) < b_t(c) \end{cases} \quad (53)$$

## K CLASS DISTRIBUTION SHIFT

We now report the results for the class distribution shift obtained by applying the mini-batch sampling procedure described in Section B. For each dataset, we choose to illustrate 3 different distributions: the one corresponding to the original labels (“Node”), the one obtained by applying both *Step 1* and *Step 2* described in the mini-batch paragraph of Section 4.2 and the one obtained by only applying *Step 2*.

### K.1 FIGURE - NODE HOMOPHILY

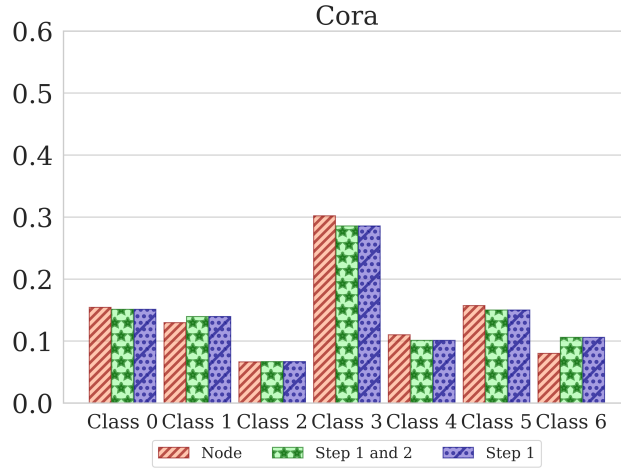


Figure 15: Class distribution for Cora

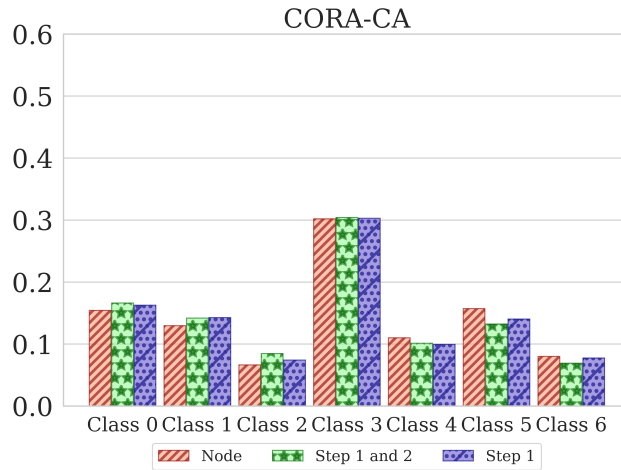


Figure 16: Class distribution for CORA-CA

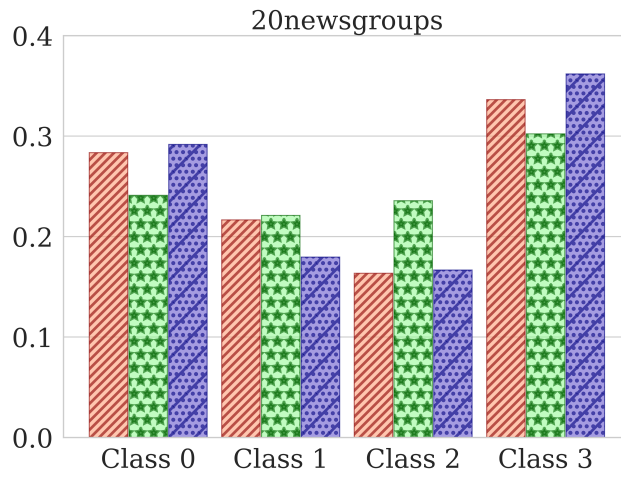


Figure 17: Class distribution for 20Newsgroup

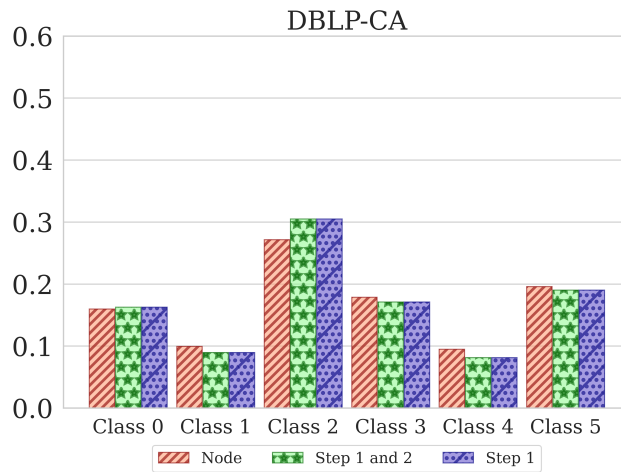


Figure 18: Class distribution for DBLP-CA

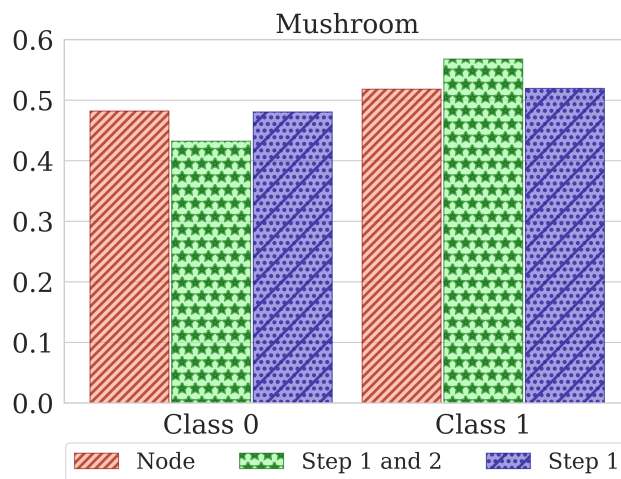


Figure 19: Class distribution for Mushroom

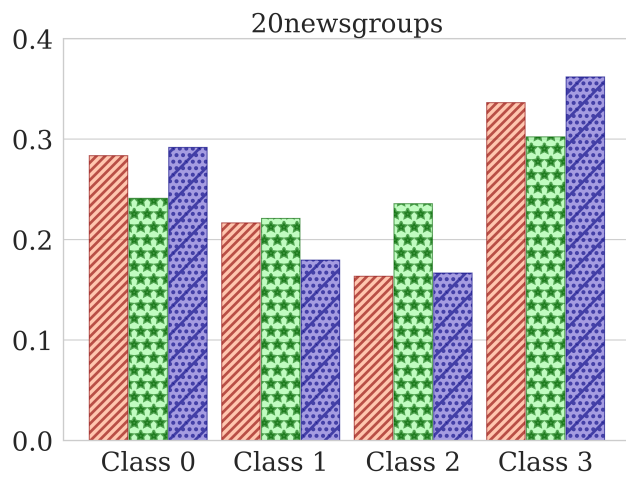


Figure 20: Class distribution for 20NewsW100